Check for updates

EVOLUTIONARY BIOLOGY

Macroevolutionary dynamics and predictors of tropical rain forest plant diversity

Laura Holzmeyer[1]*†, Francis J. Nge[1,2]†, Susana Arias Guerrero[3], Kate E. Armstrong[4], Márcio L. Bazante[5], Roxali Bijmoer[3], Renata Borosova[6], David D. Bruy[7,8], Pasakorn Bunchalee[9], Tanawat Chaowasku[10], Lars W. Chatrou[3,11], Junhao Chen[12,13], Léo-Paul M. J. Dagallier[1,4], Anissara Damthongdee[10], Roy H. J. Erkens[3,14], Federico Fabriani[11], Luiz H. M. Fonseca[11], Myriam Gaudeul[15], Paul H. Hoekstra[3], David M. Johnson[16], Thea Lautenschläger[17,18], Charan Leeratiwong[19], Ming-Fai Liu[20], Adriana A. Q. Lobão[21], Jenifer C. Lopes[22], Cedric Mariac[1], Maria F. Martínez-Velarde[23,24], Kathryn P. Mercier[25], Fabian A. Michelangeli[4], Rommel Montúfar[26], Jérôme J. Munzinger[7], Nancy A. Murray[16], Andrés E. Ortiz-Rodriguez[27], Álvaro J. Pérez[28], Michael D. Pirie[29], Heimo Rainer[30], Mijoro Rakotoarinivo[31], Carlos Rodrigues-Vaz[1,15], Germinal Rouhan[15], Hervé Sauquet[2], Bonaventure Sonké[32], Vincent R. C. Soulé[1], Tariq Stévart[33], Serafin J. R. Streiff[1], Joeri S. Strijk[34], Delphine Tardif[35], Daniel C. Thomas[12,36], Archimède Towe Patipe[1], Jan J. Wieringa[3,37], J. Nicolás Zapata[38,39], Pierre Sepulchre[35], Fabien L. Condamine[40], Thomas L. P. Couvreur[1,3]*

Copyright © 2026 The Authors, some rights reserved; exclusive licensee American Association for the Advancement of Science. No claim to original U.S. Government Works. Distributed under a Creative Commons Attribution NonCommercial License 4.0 (CC BY-NC).

Tropical rain forest is the most diverse terrestrial biome, yet the drivers of its diversification across space and time remain poorly understood. Although heterogeneous diversification rates, including both ancient and recent radiations, have been reported, these dynamics have rarely been examined within a single lineage across deep evolutionary timescales. Here, we reconstruct a dated phylogenomic tree of the pantropical plant family Annonaceae, sampling 2045 species (~82% of its diversity) and spanning ~100 million years of evolutionary history. Diversification dynamics vary markedly across tropical regions, correlated with distinct environmental factors rather than uniform processes. Sea level fluctuations dominate in the Asia-Pacific, whereas paleotemperature shapes diversification in the Afrotropics and Neotropics. We also detect a Late Cretaceous increase in diversification, indicating that a substantial portion of Annonaceae diversity originated before the Cretaceous-Paleogene boundary. Together, these results highlight how regional environmental trajectories have shaped the assembly of a diverse tropical plant family over deep evolutionary time.

INTRODUCTION

Understanding the evolutionary processes that have generated Earth's diversity is a central question in evolutionary biology. The tropical rain forest (TRF) biome harbors around half of all vascular plant species while covering only about 7% of the planet's land surface (*1*). In its modern form, TRF is a multilayered, angiosperm-dominated ecosystem occurring in regions of high precipitation and minimal temperature seasonality (*2*). Despite its profound ecological and climatic importance, the predictors of TRF diversification across space and time remain incompletely understood.

Past phylogenetic studies have shown that diversification in TRF plant lineages is not uniform but instead characterized by heterogeneous dynamics, with both ancient and more recent radiations documented across different plant clades (*3*, *4*). However, these patterns have typically been inferred from lineages with differing temporal scales, geographic distributions, and ecologies, often with limited

[1]DIADE, Université de Montpellier, CIRAD, IRD, Montpellier, France. [2]National Herbarium of New South Wales, Botanic Gardens of Sydney, Mount Annan, Australia. [3]Naturalis Biodiversity Center, Leiden, Netherlands. [4]New York Botanical Garden, Bronx, NY, USA. [5]Centro de Biociências, Departamento de Botânica, Universidade Federal de Pernambuco, Recife, Brazil. [6]Science Directorate, Royal Botanic Gardens Kew, Richmond, UK. [7]AMAP, Univ Montpellier, IRD, CIRAD, CNRS, INRAE, Montpellier, France. [8]AMAP, IRD, Herbier de Nouvelle-Calédonie, Nouméa, New Caledonia. [9]Department of Biology, Faculty of Science, Mahasarakham University, Maha Sarakham, Thailand. [10]Herbarium, Department of Biology, Faculty of Science, Chiang Mai University, Chiang Mai, Thailand. [11]Department of Biology, Ghent University, Ghent, Belgium. [12]Singapore Botanic Gardens, National Parks Board, Singapore, Singapore. [13]Department of Biological Sciences, National University of Singapore, Singapore, Singapore. [14]System Earth Science, Faculty of Science and Engineering, Maastricht University, Venlo, Netherlands. [15]Institut de Systématique, Evolution, Biodiversité (ISYEB), Muséum National d'Histoire Naturelle, CNRS, Sorbonne Université, EPHE, Université des Antilles, Paris, France. [16]Department of Biological Sciences, Ohio Wesleyan University, Delaware, OH, USA. [17]Botanical Garden, Universität Hamburg, Hamburg, Germany. [18]Chair of Botany, TU Dresden, Dresden, Germany. [19]Division of Biological Science, Faculty of Science, Prince of Songkla University, Hat Yai, Songkhla, Thailand. [20]Flora Conservation Department, Kadoorie Farm & Botanic Garden, Hong Kong SAR, China. [21]Instituto de Biologia, Universidade Federal Fluminense, Niterói, Brazil. [22]Department of Organismic and Evolutionary Biology, Harvard University Herbaria, Cambridge, MA, USA. [23]Posgrado en Ciencias Biológicas, Instituto de Biología, UNAM, Ciudad de México (CDMX), México. [24]Departamento de Botánica, Instituto de Biología, UNAM, Ciudad de México (CDMX), México. [25]Department of Biology, City College of New York, New York, NY, USA. [26]WasiLab, Pontificia Universidad Católica del Ecuador, Quito, Ecuador. [27]Departamento de Botánica, Instituto de Biología, Universidad Nacional Autónoma de México, Ciudad Universitaria, Ciudad de México (CDMX), México. [28]Herbario QCA, Facultad de Ciencias Exactas, Naturales y Ambientales, Pontificia Universidad Católica del Ecuador, Quito, Ecuador. [29]University Museum, University of Bergen, Bergen, Norway. [30]Department of Botany, Natural History Museum Vienna, Vienna, Austria. [31]Mention Biologie et Ecologie Végétales, Faculté des Sciences, Université d'Antananarivo, Antananarivo, Madagascar. [32]Department of Biology, Higher Teachers' Training College, University of Yaoundé I, Yaoundé, Cameroon. [33]Africa and Madagascar Department, Missouri Botanical Garden, St. Louis, MO, USA. [34]Alliance for Conservation Tree Genomics, Kuala Lumpur, Malaysia. [35]Laboratoire des Sciences du Climat et de l'Environnement, LSCE/IPSL, CEA-CNRS-UVSQ, Université Paris-Saclay, Gif-sur-Yvette, France. [36]Nanyang Technological University, Singapore, Singapore. [37]IBED, University of Amsterdam, Amsterdam, Netherlands. [38]The Pringle Herbarium, Department of Plant Biology, University of Vermont, Burlington, VT, USA. [39]Herbario QCA, Facultad de Ciencias Exactas, Naturales y Ambientales, Pontificia Universidad Católica del Ecuador, Quito, Ecuador. [40]CNRS, Institut des Sciences de l'Évolution de Montpellier, Université de Montpellier, Montpellier, France.
*Corresponding author. Email: laura.holzmeyer@gmail.com (L.H.); thomas.couvreur@ird.fr (T.L.P.C.)
†These authors contributed equally to this work.

Downloaded from https://www.science.org on October 08, 2026

species sampling or phylogenetic resolution (*3*–*8*). As a result, it remains hard to compare meaningfully regional diversification dynamics from deep time to the present.

A key unresolved question is how diversification dynamics vary across tropical regions and the extent to which these differences reflect distinct environmental and geological histories. Although TRF are often treated as a single biome, the Afrotropics, Neotropics, and Indo-Australian regions have experienced markedly different trajectories of climatic change, tectonic activity, and landscape evolution over the past 100 million years (*2*). These contrasting histories are expected to have shaped diversification by influencing opportunities for dispersal, isolation, and ecological specialization (*9*, *10*), such that similar levels of present-day species richness may arise from different evolutionary processes. However, most previous studies have focused either on single regions (*11*) or on global-scale analyses based on low-resolution phylogenies (*9*, *12*), limiting direct comparisons across the tropics within a unified framework. Addressing this gap requires integrating diversification dynamics across deep and recent timescales while explicitly accounting for environmental and geological variables (*13*). Factors such as paleotemperature, sea level fluctuations, and tectonic events can influence speciation and extinction by altering habitat availability, connectivity, and niche stability (*2*, *11*, *14*–*17*). However, their relative importance likely varies among regions, resulting in distinct diversification trajectories.

A related question concerns when angiosperms came to dominate TRF ecosystems. The prevailing view, inferred mainly from Neotropical paleoecological data, suggests that angiosperm ecological dominance was established after the Cretaceous-Paleogene [K-Pg, 66 million years (ago) (Ma)] mass extinction, when the collapse of gymnosperm-dominated systems created new ecological opportunities (*18*, *19*). However, many angiosperm lineages, including key tropical plant families, originated before the K-Pg boundary (*4*, *20*, *21*), and angiosperm-dominated tropical ecosystems have been documented in the Late Cretaceous (*2*, *22*). This raises the question of how much early angiosperm lineages contributed to tropical forest diversity before the K-Pg. In addition, inferring diversity dynamics through time from lineage-through-time (LTT) plots based on extant-only phylogenies suffers from identifiability issues (*23*) and consistently produces an apparent increase in diversity toward the present, a pattern often inconsistent with the fossil record (*24*). Integrating fossil evidence with molecular phylogenies therefore offers a more robust framework for inferring lineage diversification dynamics over deep to recent times (*25*, *26*).

Here, we reconstruct a densely sampled, time-calibrated phylogenomic tree of the diverse pantropical plant family Annonaceae (custard-apple plant family, Magnoliales) and integrate fossil and environmental data to investigate diversification dynamics from the Late Cretaceous to the present. Using this framework, we test how diversification rates vary across major tropical regions and evaluate the environmental and geological predictors underlying these differences while also assessing the timing and magnitude of diversification relative to the K-Pg boundary. Annonaceae provides a powerful model system for understanding TRF diversification and deep time evolutionary processes. With 2506 described species of trees and lianas (*27*), diversity is high across all major TRF regions (*28*). Hence, it consistently ranks among the most species-rich megathermal families (*2*), especially in lowland TRF, while species richness increases with increasing temperature and precipitation (*29*) tracking TRF occurrence. In addition, the Annonaceae crown node age is estimated to be Late Cretaceous [98 to 89 Ma (*20*, *21*, *30*, *31*)] and is therefore pertinent for inferring both pre– and post–K-Pg macroevolutionary dynamics. Last, decades of systematic research have led to strong taxonomic and phylogenetic knowledge (*27*), a rare feature for a TRF plant family of this size and distribution, minimizing sampling biases that often compromise comparable studies in hyperdiverse tropical groups.

RESULTS

Robust species-level time tree of Annonaceae

Leveraging our taxonomic knowledge with extensive sampling from herbarium specimens (65% of species), we successfully sequenced up to 469 Annonaceae-specific nuclear genes for all 108 genera and 2045 species or ~82% of total Annonaceae diversity (for vouchers and associated BioSample numbers see data S1). Using this data, we built a fossil-calibrated (table S1) phylogenomic timetree (Fig. 1 and fig. S1) following a backbone-and-patch approach (*32*) by dividing our sequenced species into 18 monophyletic patches. The median within-genus sampling was of 96% (range: 30 to 100%; table S2). Resolution was high across the 18 patches with an average of 88.5% of nodes with bootstrap > 75 based on the RAxML concatenated analysis and 86.8% of nodes with a local posterior probability > 0.9 for the ASTRAL species-tree analyses (table S3). The maximum clade credibility (MCC) tree of Annonaceae indicated a Late Cretaceous origin of Annonaceae (mean crown node age: 93 Ma, range: 89 to 101 Ma), with the stem node dated to the Aptian (109 Ma; 99 to 121 Ma), congruent with previous phylogenetic studies (*8*, *20*, *21*, *31*). Extant lineages representing the four Annonaceae subfamilies diverged during the Paleogene between 60 and 28 Ma (Fig. 1), while the origins of the seven largest genera (>100 species) are dated to the Oligocene and Early Miocene, between 30 Ma (*Xylopia*, crown node range: 20 to 40 Ma) and 14 Ma (*Guatteria*, crown node range: 10 to 19 Ma). This level of completeness and unprecedented resolution for a pantropical TRF plant family enabled the inference of its diversification history across the tropics.

Rate heterogeneity across the Annonaceae tree of life

We undertook a number of macroevolutionary analyses to test for rate variation. The branch-specific time-dependent model of diversification (CLaDS2) uncovered substantial diversification-rate heterogeneity with numerous changes in speciation rates along the branches, especially in younger lineages, whereas deeper branches showed more uniform dynamics (Fig. 1).

The heterogeneity detected in our analyses was supported by three significant clade-based increases [Bayesian Analysis of Macroevolutionary Mixtures (BAMM)] in diversification rate occurring from 32 Ma onward (Fig. 1, nodes 1 to 3), followed by diversification slowdowns toward the present (fig. S2). These shifts should be interpreted as indicative of broad-scale changes in diversification rates supporting rate heterogeneity rather than precise estimates of the number or exact placement of rate shifts. The first rate shift (~647 species; crown age ~25 Ma, node 1) was detected at the stem node of a large mainly Southeast Asian clade (Miliuseae and allied tribes). The second rate shift (~440 species; crown age ~28 Ma, node 2) was detected at the crown node of the mainly lianescent tribe Uvarieae. Last, we also detected a significant rate shift at the stem node of the diverse Neotropical tree genus *Guatteria* (~185 species; crown age ~14 Ma, node 3). Rate heterogeneity was also confirmed when using identifiable rates

Downloaded from https://www.science.org on October 08, 2026

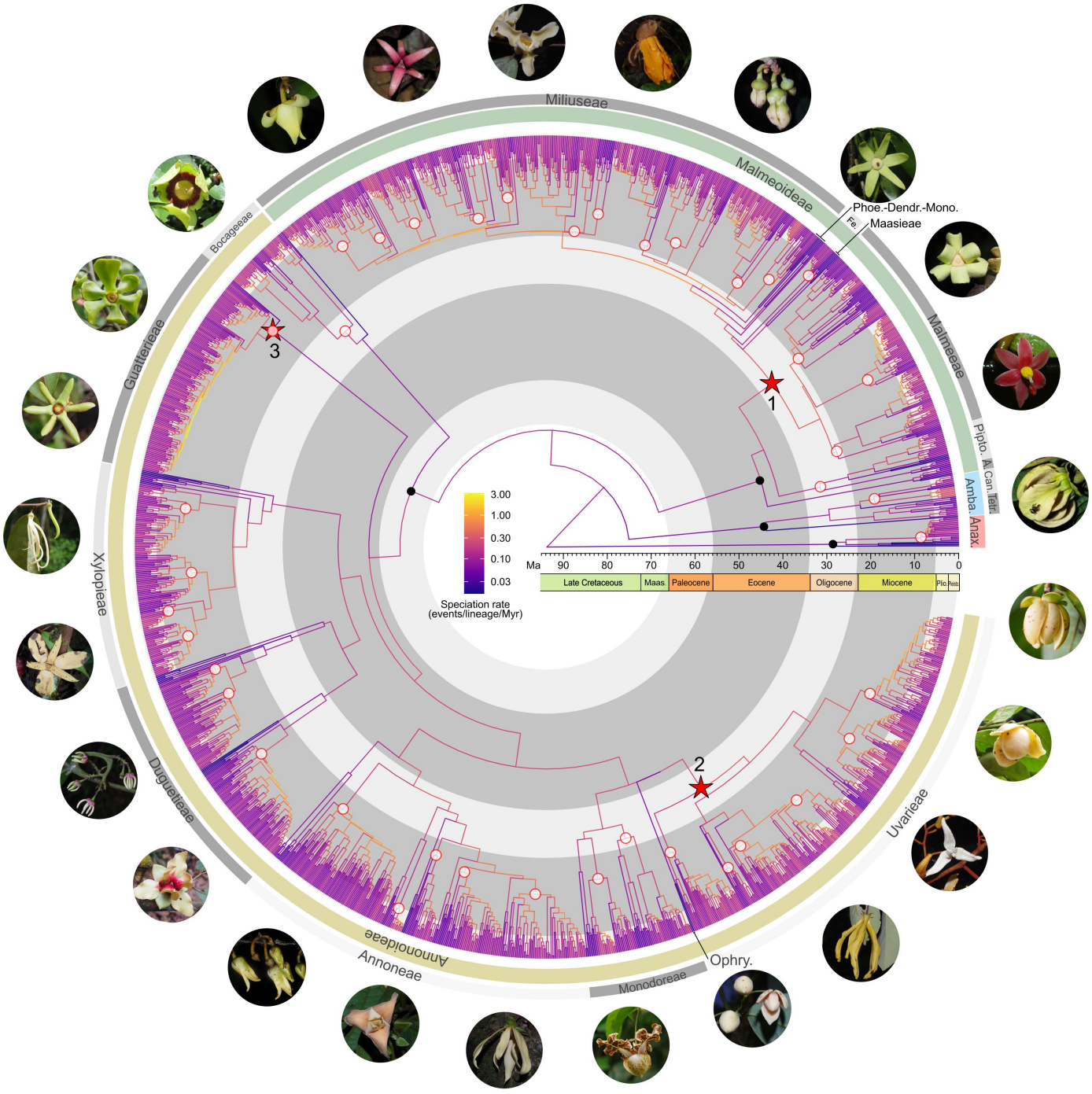


Fig. 1. Time-calibrated species-level phylogenomic tree of Annonaceae. All subfamilies, tribes, subtribes, and genera included with 82% of species sampled of the 2506 described species. Branch colors represent net speciation rates estimated from the CLaDS2 model (purple = low, red = intermediate, and yellow = high). Red stars indicate location of significant rate shifts detected using Bayesian Analysis of Macroevolutionary Mixtures (BAMM) at the crown node leading to the Southeast Asian and Neotropical clades of Malmeoideae (1), at the crown of tribe Uvarieae (2), and the crown node of the genus *Guatteria* (3). Black circles indicate the crown nodes of the four Annonaceae subfamilies. Light red circles represent the crown nodes of the 40 geoclades used in this study. Photos of Annonaceae from T.L.P.C. Amba., Ambavioideae; Anax., Anaxagoreoideae; Can., Canangeae; Dendro., Dendrokingstonieae; Fe., Fenerivieae; Mono., Monocarpieae; Ophry., Ophrypetaleae; Phoe., Phoenicantheae; Pipto., Piptostigmateae; Tetr., Tetramerantheae; Maas., Maastrichtian.

Downloaded from https://www.science.org on October 08, 2026

(*23*), which showed variable pulled diversification rates (PDR) with periods of both positive and negative rates over the past 60 million years (Myr), ending with an increase toward the present (fig. S3). These differences in apparent temporal trends relative to model-based approaches arise because PDR summarize information from extant-only phylogenies, whereas methods such as BAMM infer diversification dynamics using explicit models of branching-rate variation through time.

We also detected shifts among alternative birth-death diversification regimes at the major clades (subfamilies and tribes) thus following different evolutionary trajectories rather than a single family-wide pattern (fig. S4A), further supporting variable diversification patterns. The best-fitting model for the family backbone was a variable-birth and constant-death model (BVAR-DCST), while the backbone of the Malmeoideae followed a constant birth-death model (BCST-DCST). We inferred a high speciation rate at the start suggesting an early-on high diversification rate followed by declining rates (fig. S4B), in agreement with several other analyses conducted here using different approaches (see below). All remaining detected shifts in birth-death models indicated tribes shifting to pure-birth models—either constant (BCST; 5 tribes) or time-varying (BVAR; 10 tribes) with extinction no longer detected.

Last, we found a significantly negative gamma statistic [$\gamma = -21.5^{***}$ ($P < 0.01$)] with posterior trees having a γ between -14 and -19 ($P < 0.01$). The gamma (γ) statistic tests for departures from constant-rate diversification, with negative values indicating an excess of early branching events. These results suggest that more branching events were significantly clustered toward the stem of the MCC and posterior trees, further indicating early radiation. We also calculated the gamma statistic for five fully sampled extant time trees extracted from the modeled complete phylogenies of the INSANE analysis (see Supplementary Materials and Methods). The gamma statistic remained significantly negative (min: -20.63; max: -16.92) even under a hypothesis of complete sampling.

Fossil record and inference of extinction rates

Using literature, we compiled a list of 124 Annonaceae fossil occurrences representing 107 taxa (data S2). The oldest fossil assigned to Annonaceae is *Futabanthus asamigawaensis* (*33*) dated to the Early Coniacian (86.3 to 89.8 Ma). Of the 124 fossils, 65 are based on leaf imprints, 2 on pollen, 49 on seeds, 4 on wood anatomy, and 3 on a fruit imprint. A total of 98 (91%) occurrences was represented by singletons (table S4), which is a taxon represented by a single occurrence, which creates problems for extinction rate inferences (see Materials and Methods). Thus, we complemented our Annonaceae dataset with fossils assigned to Magnoliales in general, the order to which Annonaceae belongs. We assume here that extinction rate estimates are comparable with other characteristic rain forest families such as Myristicaceae and Magnoliaceae with low diversity outside of the tropics. This added 122 fossil occurrences. The final Magnoliales dataset (including Annonaceae) contained 243 fossil occurrences in 157 taxa across 119 Myr (fig. S5). The level of singletons was lowered to 78% (115 occurrences; table S4).

The time-variable Poisson process (TPP) model best fit the fossil preservation data and revealed three major shifts in preservation rates at ~66, 33.9, and 23 Ma. We therefore retained only these supported shifts in the final TPP analysis to avoid overfitting. All replicate runs from PyRate provided the same overall trend for the evolution of extinction rates through time (fig. S6). However, there were differences of rate intensity between epochs. Overall, there were three main periods of increased extinction: Maastrichtian, Early Eocene, and Late Miocene. Replicates differed most in their extinction rates during the Eocene with either decreasing rates or a mixture of increasing and decreasing rates through time. All replicates detected a decrease of extinction during the Pliocene and an increase during the Pleistocene.

Diversification and diversity through time

The estimated fossil-based extinction rates of the combined PyRate analyses was used in INSANE (see Materials and Methods) to simulate past diversity through time for Annonaceae. We sampled 200 modeled complete phylogenies, each including extant sampled, unsampled, and extinct lineages (Fig. 2 for one such phylogeny). The resulting diversity-through-time plots (Fig. 3A) showed a rapid increase in lineages at the origin of Annonaceae before the K-Pg boundary, after which diversity followed a waxing-and-waning evolution, with diversity increasing and decreasing through time. We also ran INSANE with extinction rates extracted from three individual PyRate replicates (j1, j3, and j8), which all returned highly congruent results (fig. S8). Last, the inferred trajectory, magnitude, and timing of diversity through time remained robust across alternative crown-age calibrations for Annonaceae (fig. S9). Initially high INSANE inferred speciation rates declined toward the K-Pg boundary, after which they fluctuated at lower levels, showing an overall negative trend (Fig. 3B). Absolute declining speciation rates were recovered irrespective of the extinction rate assumption used in the birth-death diffusion model as seen with the negative median drift parameter $\alpha = -0.25$ (fig. S12, A to D). Specific speciation rates of extant lineages remained high for the first half of Annonaceae evolution (Fig. 3C), reaching a peak during the middle of the Eocene and then around the mid-Miocene climate optimum (MMCO). The first lineage rate declines started around the Eocene-Oligocene transition (EOT; 33 Ma), with all lineages undergoing declines after the MMCO.

Last, on the basis of our extant phylogeny, we detected three main periods of possible mass extinction affecting Annonaceae diversification (Fig. 3B). Strong support [Bayes factor (BF) > 6] for a range survival probabilities (5 to 25%) was detected around the EOT, while decisive support (BF > 10) was detected at 22 Ma (25%) and 14 Ma (10 to 25%).

Environmental predictors of diversification

We used RPANDA as an exploratory comparative framework to investigate which environmental factors are correlated with Annonaceae diversification by selecting 40 geographically defined clades (referred to as "geoclades"), each concentrated in one of three major tropical regions (Asia-Pacific, South and Central America, and Africa, including Madagascar and the Mascarenes; Fig. 1 and table S5). Using the birth-death environment-dependent model implemented in RPANDA, 34 of the 40 geoclades (85%) showed significant associations with one or several of the environmental factors tested (Fig. 4, table S5, and data S3 for full results). For the remaining six geoclades, four African and two South American, time-dependent models provided the best fitting model. These latter cases were generally favored in younger and species-poorer geoclades, but this was rarely statistically significant (fig. S11). In the Asia-Pacific region, sea level fluctuation was positively associated with diversification in 88% of geoclades (14 geoclades; data S3). In South and Central America, regional temperature was overall the best-fitting predictor in eight geoclades

Downloaded from https://www.science.org on October 08, 2026

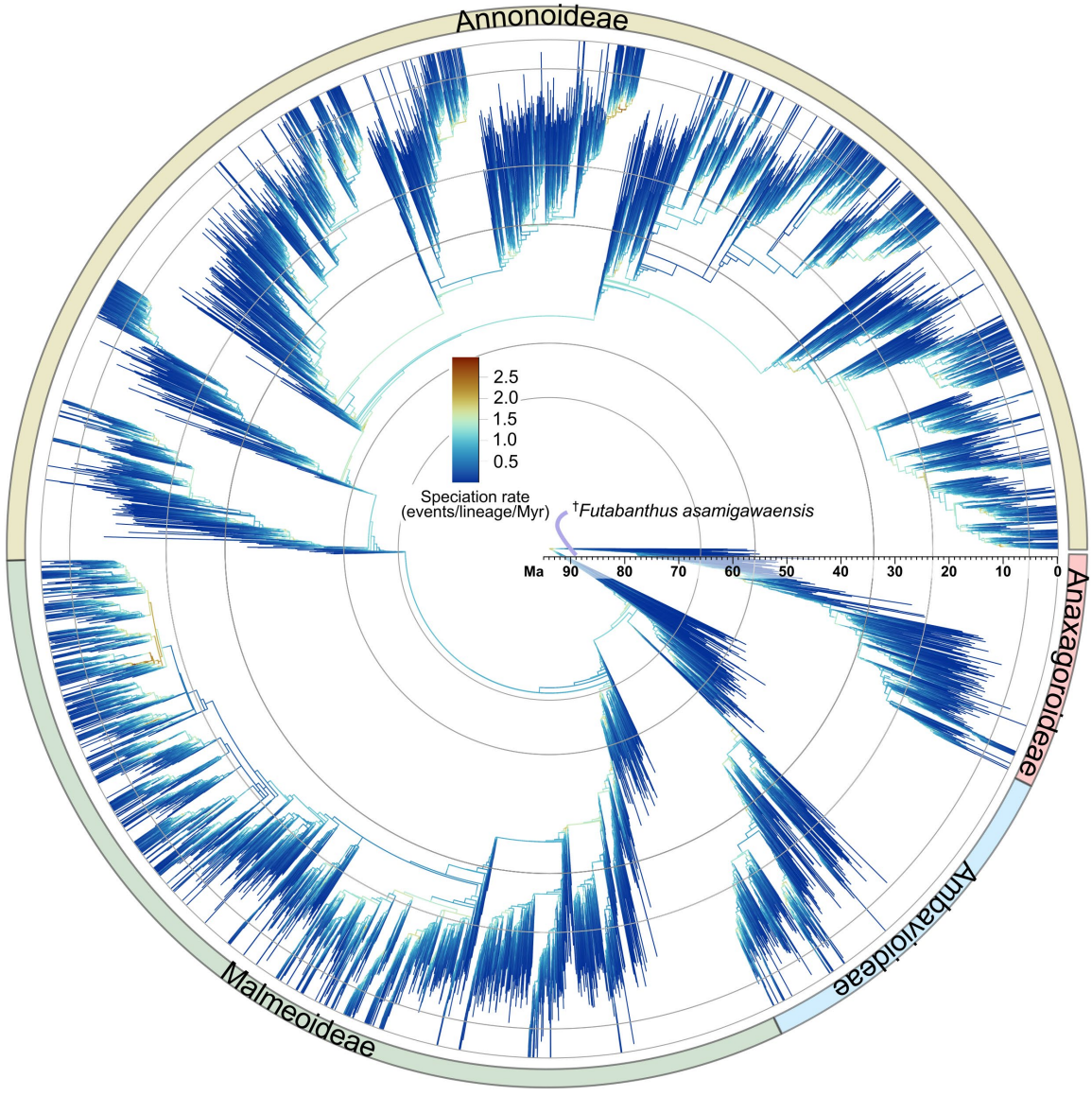


Fig. 2. Modeled complete phylogeny of Annonaceae. One of the 200 augmented posterior trees (tree #15) of Annonaceae incorporating extant, extinct, and unsampled species modeled using the birth-death diffusion posterior and fossil informed extinction rate. Inferred speciation rate visible on the branches; warmer-red colors represent higher rates. The fossil *F. asamigawaensis* has been used to calibrate the crown node of Annonaceae. Speciation rates inferred from INSANE are not directly comparable to those of Fig. 1 (using ClaDS2), due to differences in model assumptions and data integration.

(67%; data S3). The Caribbean-centered geoclade, *Xylopia* A, was associated with sea level change (ωAIC = 0.765; data S3). The diversification of the only Central American–centered geoclade (*Desmopsis* clade) was correlated with continental fragmentation (ωAIC = 0.966; data S3), and the single North American geoclade was negatively associated with North American temperature change (ωAIC = 0.620; data S3). Last, in the Afrotropics, diversification was positively correlated with regional temperature in 60% of geoclades (six geoclades; table S5 and data S3).

DISCUSSION

We generated the largest dated phylogenomic tree for any major tropical plant family to date, sampling up to 469 nuclear genes and 2045 species (82% of total diversity) and covering all major TRF regions (Fig. 1). This level of taxonomic and geographic coverage, far exceeding previous efforts in the family (*8*), offers an in-depth perspective in a major pantropical plant family and its implications for the evolution of the TRF biome. These results are complementary to recent large-scale phylogenomic studies of TRF animal clades (*34*). By integrating our phylogenomic framework with the fossil record and state-of-the-art macroevolutionary methods, we reconstructed the diversity dynamics of Annonaceae from deep to recent time. Our results reject both constant-rate and purely time-dependent models, revealing instead that present-day Annonaceae diversity reflects a complex interplay of ancient and recent diversification bursts, waxing-and-waning diversity dynamics, and extinction events correlated with regional environmental change.

Downloaded from https://www.science.org on October 08, 2026

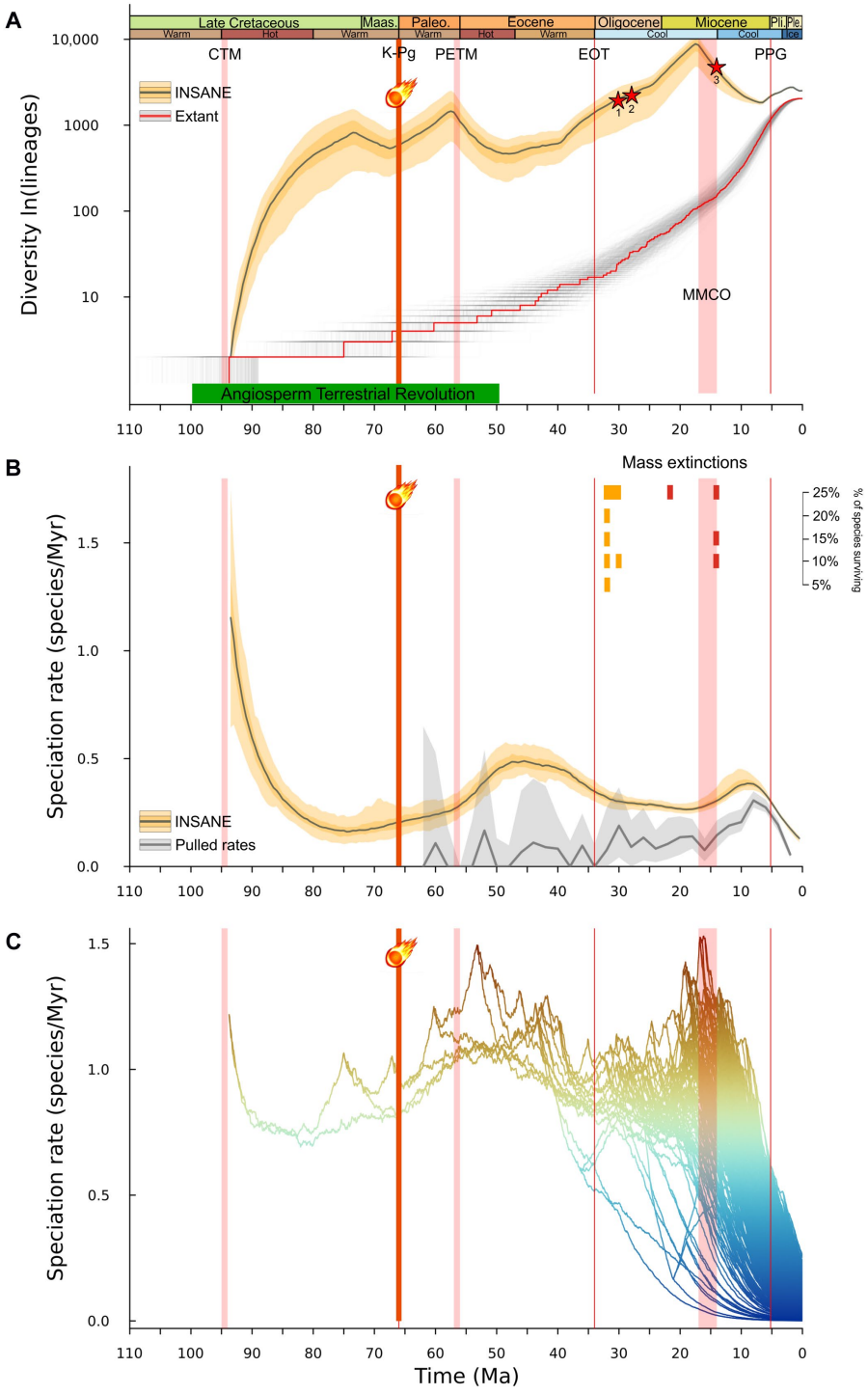


Fig. 3. Early burst followed by decelerating speciation and waxing-and-waning diversity dynamics of Annonaceae. (**A**) Log number of lineages (diversity) through time of Annonaceae modeled on the basis of Bayesian data augmentation under a birth-death diffusion model with time-varying extinction rates estimated from the fossil record. The solid black line shows the median number of lineages (diversity); the shaded orange regions indicate the 50% credible interval of 200 posterior trees. LTT plots obtained from the extant-only time trees shown in red (MCC tree) and gray lines (500 posterior trees). Red stars represent significant shifts in diversification rates inferred using BAMM as shown in Fig. 1. World climate states (hot, warm, cold, and ice states) following (*51*). (**B**) Estimated speciation rates for Annonaceae based on 200 posterior complete modeled trees (yellow) from 95 Ma onward and the pulled speciation rate (PSR) based on extant-only MCC time tree (gray) over the past 60 Myr. Inset is the timing of possible mass extinction events based on the extant tree for different percentages of surviving lineages (25 to 5%) inferred using Compound Poisson process on Mass-Extinction Times (CoMET) {orange: strong support [Bayes factor (BF) > 6]; red: decisive support (BF > 10)}. (**C**) Lineage-specific speciation rate inferred from 200 posterior complete modeled trees with extinct species removed. CTM, Cretaceous Thermal Maximum; PETM. Paleocene-Eocene Thermal Maximum; PPG., Pliocene-Pleistocene glaciations; Pli., Pliocene; Ple., Pleistocene.

Downloaded from https://www.science.org on October 08, 2026

Ancient and recent rate-variable diversity dynamics

In contrast to the constant accumulation hypothesis, Annonaceae species richness is explained by variable diversification rates, including both early and recent diversification bursts across lineages and through time (Figs. 1 to 3). This conclusion is not affected by identifiability issues (*23*) because extant-only estimated pulled rates were also highly heterogeneous, with intervals of both positive and negative diversification rates (fig. S3). Similar patterns were recovered from modeled complete phylogenies (Fig. 2) based on fossil-informed augmentation (Fig. 3, A and B). In addition to rate heterogeneity, we show that present-day Annonaceae diversity is the result of different distinct evolutionary regimes with multiple shifts to different modes of diversification during its evolutionary history (fig. S4A). Our results contrast with constant diversification scenarios as inferred for example in Neotropical birds using similar densely sampled phylogenetic approaches (*34*). The differing diversification dynamics between vertebrate and plant lineages suggest that plant-focused studies provide a complementary perspective on the assembly of TRF diversity (*11*).

Overall rate heterogeneity was punctuated by three significant clade-based increases in diversification rates from 30 Ma onward supporting the heterogenous hypothesis (Fig. 1, nodes 1 to 3, and fig. S2). However, we note that apparent rate shifts close to the present are easier to detect based on a greater density of branching events in the shallow parts of the tree (*35*), although our result also holds under the fossil-informed modeled complete phylogenies (uptick in speciation around 10 Ma; Fig. 3B). This result was also recovered in several other phylogenetic studies of TRF clades (*6*, *8*, *36*, *37*) but not always (*38*). These shifts are possibly linked to key innovations or ecological opportunities known to affect diversification in other major TRF plants (*39*). Notably, the rate shift at the crown node of the species-rich Neotropical tree genus *Guatteria* (Fig. 1, node 3) exemplifies recent and rapid speciation in Amazonia (*3*, *5*, *8*), while the evolution of the lianescent habit may have influenced diversification in the mainly climbing tribe Uvarieae (*40*). In Southeast Asia, the diversification shift in Miliuseae and related tribes (~647 spp.; ~25 Ma) likely reflects ecological opportunities associated with dispersal and radiation across the Indo-Australian Archipelago (*41*).

In parallel, our extant-only tree analyses also supported the "early burst" hypothesis, revealing rapid initial lineage diversification followed by a gradual slowdown through time. This pattern was robust to both dating uncertainty and taxon sampling biases (fig. S9 and γ statistic $\ll -2.0$) and was also recovered when inferring diversity through time (see below). In addition, a similar pattern was detected for the backbone of the extant phylogeny, indicating a high diversification in the Late Cretaceous before declining (fig. S4B). These results align with other TRF phylogenetic studies reporting an early burst scenario (*4*, *42*) and with trends observed across angiosperms more broadly (*21*), although such signals are often difficult to recover from extant-only phylogenetic trees.

Waxing-and-waning evolution of TRF diversity

Given the limitations of extant-only phylogenetic analyses, we used a Bayesian data augmentation approach that integrates our densely sampled extant phylogenetic tree with fossil-based extinction rate estimates (data S2) (*26*) to simulate complete phylogenies and infer deep to recent time diversity dynamics.

Going beyond rate heterogeneity, we show that Annonaceae followed a waxing-and-waning model with repeated cycles of increases and decreases of diversity since the mid-Cretaceous (Fig. 3A), consistent with our PDR estimates (fig. S3A). These patterns are not expected to match exactly, as they are inferred from different data sources and statistical frameworks. PDR summarize the identifiable temporal signal in the extant-only phylogenies (*23*), whereas fossil-informed augmented trees reconstruct diversity dynamics by explicitly incorporating extinction and missing lineages (*26*). Moreover, extinction rates were estimated from the broader Magnoliales fossil record, thus the resulting diversity trajectories are conditional on the assumption that these order-level estimates are informative for Annonaceae, which remains to be tested. This result contrasts with previous studies that inferred constant accumulation of major plant lineages in deep time based on less densely sampled, extant-only phylogenies (*6*, *42*, *43*), providing a much more detailed view of TRF diversity evolution. These diversity cycles are consistent with local fossil-based TRF paleodiversity dynamics during the Cenozoic (*2*, *44*) and is, to our knowledge, the first time it is inferred for a pantropical TRF plant lineage. Furthermore, the fossil-based estimated extinction rates for the largely tropical order Magnoliales were always positive and highly variable across the different epochs since the mid-Cretaceous (fig. S7), refuting the hypothesis that TRF-centered clades might have evolved constantly under zero or negligible extinction rates (*45*).

Using our fossil-informed modeled complete phylogenies, we show that diversity increased rapidly (Fig. 3A) during the Late Cretaceous (95 to 75 Ma), with Annonaceae reaching a substantial fraction of its present-day species richness by then. This further supports the early burst hypothesis as explained above. Although quantifying absolute past diversity remains challenging especially at the angiosperm scale due to fossil limitations (*19*), our results benefit from focusing on a single, well-circumscribed and ecologically homogeneous TRF family with exceptionally dense extant sampling. This makes diversification estimates for Annonaceae far more reliable than comparable attempts across angiosperms as a whole, where sampling heterogeneity and low resolution greatly hinder credible inferences. Thus, while the precise numerical values of our diversity curves should be interpreted cautiously, the signal of a major Late Cretaceous diversification pulse is consistently recovered across the sensitivity analyses conducted within this fossil-informed framework.

Furthermore, these phases of diversity increases and declines are consistent with established periods of TRF evolution (*2*). After a decline during the Maastrichtian, diversity rebounded after the K-Pg event, driven by a steady increase in speciation rates (Fig. 3, A and B). We do not detect a negative impact on speciation rates across the K-Pg boundary (Fig. 3, B and C), suggesting limited global effects on TRF lineage diversification (*45*–*47*) although this event had geographically heterogeneous impacts across regions (*18*, *48*). We inferred two major Cenozoic peaks of Annonaceae diversity (Fig. 3A), each concordant with known periods of widespread TRF expansion and high overall paleodiversity. The first occurred during the Paleocene-Eocene Thermal Maximum (56 to 57 Ma), a global "golden age" of TRF diversity (*2*, *44*, *49*). The second, with inferred Annonaceae diversity reaching an all-time maximum (~10,000 species), took place during the MMCO (17 to 15 Ma), the last period when TRF extended beyond the tropics (*2*) with high species richness in Amazonia (*50*). In addition, two major diversity declines punctuated this trajectory. The first occurred during the early Eocene (55 to 45 Ma) possibly linked to global cooling (*51*) that dampened diversification (*52*). The second, in the late Miocene (15 to 7 Ma), reflects a possible severe loss of 75 to 90% of lineages around 14 Ma, as supported by strong

Downloaded from https://www.science.org on October 08, 2026

statistical evidence for a mass extinction inferred from the extant phylogeny (Fig. 3B; 2ln BF > 10). This decline coincided with intensified global cooling and the transition into the "icehouse state" (*51*), poleward glaciation, and TRF contraction to equatorial latitudes linked to increased aridification (*2*). Following this event, speciation rates rose again (Fig. 3B), peaking around 7 Ma and driving a modest recovery over the past 5 Myr, coinciding with Milankovitch-driven climatic oscillations possibly promoting diversification.

Environmental predictors of TRF diversity

Given heterogeneous diversification rates and waxing-and-waning dynamics, we tested whether Annonaceae diversification is correlated with environmental-dependent or nonenvironmental constant-rate or time-dependent models. We tested region-specific and global abiotic predictors in a regional approach by defining 40 geoclades assigned to the three major tropical regions (Asia-Pacific, Neotropics, and Afrotropics). We show that diversification across Annonaceae is predominantly correlated with environmental factors selected for this study. Time-dependent models were only best fitting in 6 (4 African and 2 South American) of the 40 geoclades (Fig. 4), suggesting that diversification in these clades cannot be fully accounted for by the selected abiotic predictors (*11*). These inferences are based on extant-only phylogenies and environment-dependent birth-death models and thus may be affected by identifiability constraints under heterogeneous extinction. Overall, our results reinforce the view that present-day Annonaceae diversity is primarily the outcome of environmental regionally distinct histories rather than constant or time-dependent processes (*12*).

In the Asia-Pacific region, the majority of clades showed a positive correlation between sea level fluctuations and diversification rates, supporting a key role of sea level change in shaping present-day biodiversity in this island-dominated and tectonically active region. Sea level changes affect speciation and extinction dynamics in an island context by directly influencing connectivity between landmasses (isolation), changing available area size (carrying capacity), and affecting dispersal frequency (*53*). Our results provide an explanation for biogeographic patterns previously inferred in the region (*54*, *55*).

In South and Central America, regional temperature was overall the best-fitting predictor for diversification rates (Fig. 4). In agreement with other studies (*50*), we show that Andean uplift is not strongly supported as a primary predictor for Annonaceae diversification, with only three geoclades showing elevation as one of their three best models (but never the best; data S3). In Amazonia, Annonaceae primarily inhabit the lowlands, and although studies have suggested a role of the Andean uplift as a predictor for diversification of some clades (*56*), our results suggest that temperature is more important overall. The Caribbean-centered geoclade, *Xylopia* A, was associated with sea level change (Fig. 4), which could be attributed to island size and connectivity dynamics similar to the Southeast Asian clades. The diversification of the only Central American geoclade (*Desmopsis* clade) was correlated with continental fragmentation (Fig. 4) possibly linked to the ongoing tectonic activity and the closure of the Panama Isthmus (*57*).

In the Afrotropics, diversification was positively correlated with regional temperature in most geoclades (Fig. 4). This supports the idea that long-term temperature fluctuations shaped diversification patterns by influencing the expansion and retraction of African TRF (*17*). Specifically, retraction and fragmentation through aridification linked to global cooling since the late Eocene may have played a key role (*2*, *17*), while warmer phases could have facilitated TRF expansion.

A Late Cretaceous radiation in Annonaceae

As discussed above, using our fossil-informed modeled complete phylogenies, we infer that diversity increased rapidly during the Late Cretaceous (95 to 75 Ma) under high initial speciation rates, reaching nearly half of its present-day richness (Fig. 3A). Thus, Annonaceae and possibly other already evolved tropical plant families were rapidly diversifying well before the Cenozoic (*4*, *42*). This interpretation is further supported by fossil evidence for the presence of angiosperm-dominated rain forests predating the K-Pg boundary, notably in Africa around 80 Ma (*22*, *46*, *58*, *59*) even if such ecosystems were not yet widespread in other tropical regions such as the Neotropics (*18*, *60*).

This diversity pulse coincides with the first half of the Angiosperm Terrestrial Revolution (100 to 75 Ma) (*19*) when some angiosperm lineages rose to ecological dominance (*61*) driven by the evolution of key functional and reproductive innovations (*62*, *63*) and intense insect-angiosperm codiversification (*64*). While this early diversification does not imply the presence of modern TRF per se during the Late Cretaceous, it indicates that already evolved angiosperm families such as Annonaceae were diversifying within these megathermal forest ecosystems. The structure and function of these Late Cretaceous forests remain debated, with some studies suggesting that Cretaceous vegetation lacked key physiological and ecological characteristics of modern TRF (for example, leaf vein density and canopy structure), implying nonanalogous forest systems (*18*, *65*). Our results therefore speak to the timing of lineage diversification rather than the establishment of modern TRF ecosystems. They provide a temporal framework to assess how early angiosperm lineages may have contributed to the assembly of modern TRF diversity across regions (*4*).

Our inference of extinction rates relies on fossil occurrence data aggregated at the level of Magnoliales and applied to our Annonaceae phylogenomic tree, thus assuming broadly comparable preservation and extinction processes across lineages. Preservation and sampling biases, however, vary not only among families but also within lineages through time, environments, and fossil types, making fully lineage-specific extinction estimates difficult to obtain from the available fossil record (*26*), especially of tropical plant clades. Although the PyRate framework explicitly models preservation and accounts for incomplete and temporally heterogeneous sampling (*66*), it does not fully resolve biases when data are aggregated at higher taxonomic levels. Notably, similar fossil occurrence counts between Annonaceae and other Magnoliales contrast with their markedly different extant diversities, suggesting uneven preservation or sampling. These limitations are inherent to fossil-based approaches, and our results should therefore be interpreted as reflecting order-level extinction signals rather than lineage-specific histories. Nevertheless, this approach enables integration of fossil information in a comparative framework and captures broad-scale temporal dynamics that would be inaccessible using extant-only data (*26*).

In conclusion, our study demonstrates how combining dense phylogenomic sampling with the fossil record can reveal complex deep to recent, lineage-specific diversification histories in tropical plants that may also be applied to other megathermal lineages. A substantial proportion of our dataset (~65%) was derived from leaves sampled from herbarium specimens, including century-old collections (as old as 1785) and type material (239 species), underscoring the

Downloaded from https://www.science.org on October 08, 2026

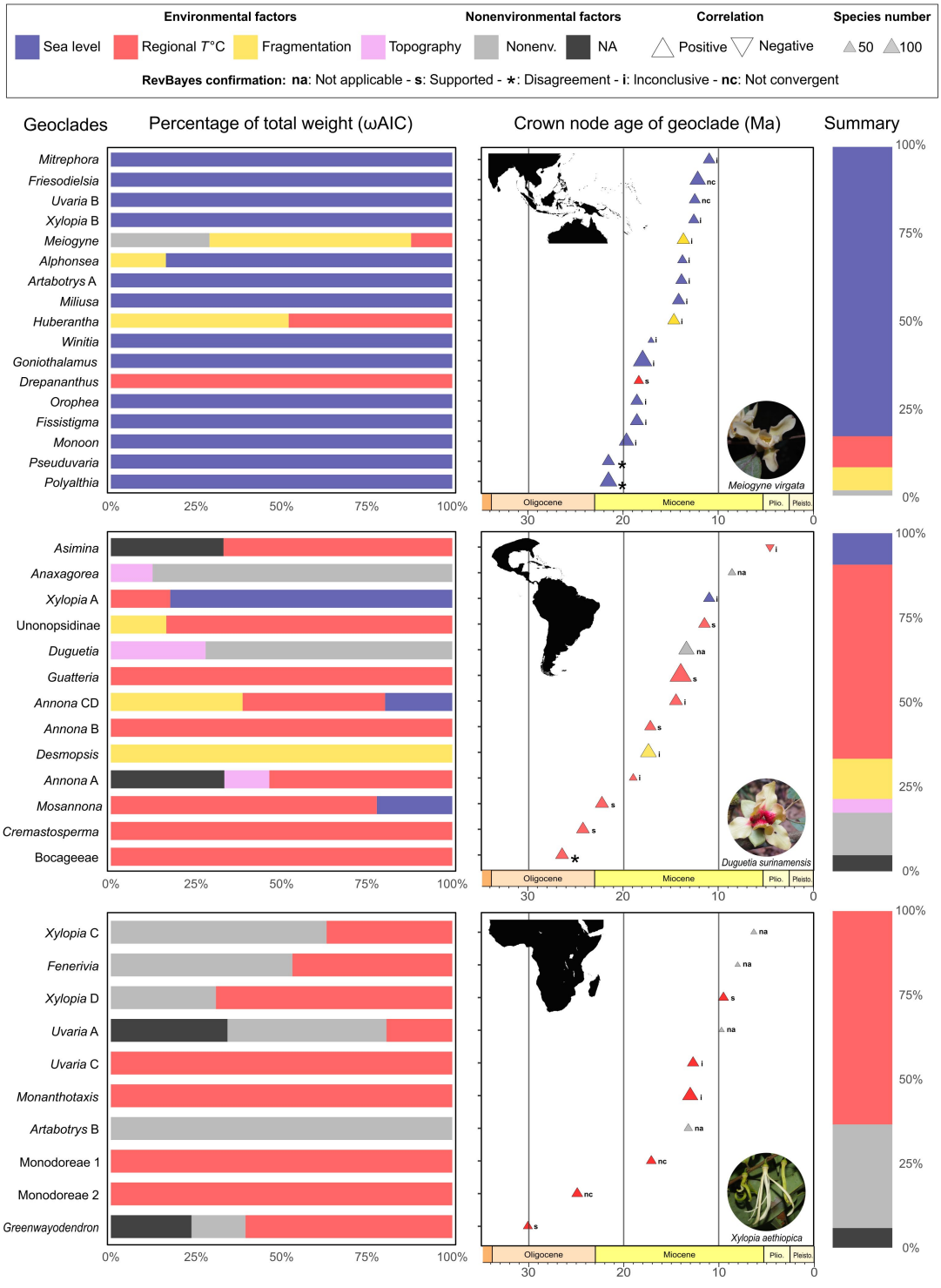


Fig. 4. The regional abiotic correlates of Annonaceae diversification dynamics. From left to right: Model-category histograms: for each geoclade, ordered from oldest (top) to youngest (bottom), bars show the model categories with the strongest support (ωAIC ≥ 0.1). The NA category indicates models that were fitted with ωAIC < 0.1. Clade-age plot: each geoclade is plotted at its mean crown node age, with the best-fitted model category indicated by color and the fitted α parameter (speciation rate correlation) given in the symbol shape, and symbol size proportional to clade size. Upright triangles denote α > 0 (positive correlation); inverted triangles denote α < 0 (negative correlation). An asterisk (*) next to a triangle indicates cases where this model assignment conflicts with Bayesian model results. Model-distribution summary: Stacked bars summarize the proportion of the best-supported model categories across all geoclades per region. RevBayes model support is indicated by four categories: supported ("s"), when results are consistent with the best RPANDA-inferred model; not supported ("*"), when an alternative model is favored; inconclusive ("i"), when no clear distinction among models can be made; and non-convergent ("nc"), when analyses failed to converge. Finally, nonenvironment RPANDA models are indicated by "na" (not applicable). Photos of Annonaceae from T.L.P. Couvreur.

Downloaded from https://www.science.org on October 08, 2026

critical role of natural history collections in enabling large-scale evolutionary research (*67*). Beyond providing access to rare and geographically dispersed hard to sample taxa, these collections also contribute essential metadata that make integrative phylogenomic analyses possible (*68*, *69*). This study further highlights the importance of sustained investment in curation, digitization, and ethical sampling practices to ensure that herbaria continue to serve as a cornerstone for global plant biodiversity research (*67*). The diversification of TRF plant diversity, as exemplified by Annonaceae, is complex and does not follow a single evolutionary model, rather its diversity reflects the collective result of both ancient and recent lineage-specific diversification histories affected by regional processes, offering a more nuanced view of TRF evolution. Future phylogenomic studies will be essential to uncover the role of additional diversification predictors, including biotic factors such as plant-pollinator interactions, herbivory, seed dispersal syndromes, and competition.

MATERIALS AND METHODS

Taxon sampling and sequencing

To standardize taxonomy across the family, we curated a checklist of all accepted Annonaceae names, based on recent taxonomic revisions and our expertise (last updated on 30 June 2024). This checklist was then used to calculate statistics used in downstream analyses (sampling fractions; Dryad DOI: 10.5061/dryad.w6m905r27). Of the 2506 accepted names at the time of this study (see Supplementary Text) we sampled 2235 species (~90%) from either field-collected leaves dried in silica gel (~35%) or leaves directly sampled from herbarium specimens (~65%) deposited in 51 herbaria. Herbarium material was prioritized to minimize new field collections. Sampling was conducted with minimal impact, with all specimens fully documented and linked to source vouchers to ensure traceability. Material access and use complied with institutional and international regulations (Convention on Biological Diversity and Nagoya Protocol), including verification of ABS status and the establishment of material transfer agreements with partner institutions. When required, additional permissions were obtained from countries of origin, and in situ collections were conducted in coordination with national authorities or local collaborators. All sampling followed recent best-practice guidelines for herbarium research (*69*), and sequencing data and associated metadata are being returned to source institutions where possible (see the Supplementary Materials for more details).

Specimens were sequenced using the 469 Annonaceae-specific nuclear probe set (*70*) following available protocols (*71*, *72*). All 108 currently accepted genera were included. We used HybPiper v1.2 (*73*) to assemble loci from the Annonaceae baiting kit (*70*). Low-quality accessions were identified using the max_overlap statistic (*74*). Specimens with max_overlap lower than 0.5 and paralogs as identified with HybPiper were excluded (table S3 and data S2). All raw sequence data for the 2045 species included in our tree are available on Sequence Read Archive under BioProjects: PRJNA508895 and PRJNA1265870 (data S2).

Molecular dating of Annonaceae patches

A species-level dated phylogenetic tree for Annonaceae was generated using a backbone-and-patch approach (*32*) following the Bayesian sequential-subtree methodology applied to generate the species-level dated tree of mammals (*75*). For the backbone, we leveraged a recently published phylogenomic analysis of magnoliids (*76*) based on the Angiosperms353 baiting kit (*77*) (Supplementary Text; tree deposited in Dryad DOI: 10.5061/dryad.w6m905r27). The data contained 235 unique species representing 199 genera and all 18 families of the orders Canellales, Laurales, Magnoliales (which includes Annonaceae), and Piperales. A total of 78 genera from across the Annonaceae family (including all subfamilies and most of the tribes) was included. Calibration was achieved using five expert-validated and phylogenetically placed (table S1) magnoliid fossils (*78*).

We divided the sequenced samples into 18 smaller monophyletic patches, ranging from 25 to 224 species to ensure computational feasibility (Supplementary Text and table S3). Each patch included at least one overlapping taxon with the backbone phylogeny for tree merging. We inferred trees from the concatenated sequence data using RAxML v8.2.9 (*79*) under GTRGAMMA with 100 bootstraps and estimated species trees assuming coalescence with ASTRAL v5.7.8 (*80*). Constrained starting chronograms based on the RAxML trees were generated with treePL v1.0 (*81*). We selected 30 clocklike loci using SortaDate (*82*). Bayesian divergence-time analyses were performed in BEAST v2.6.7 (*83*) via CIPRES (*84*), using a relaxed lognormal clock and birth-death priors, with convergence assessed in Tracer v1.6 (*85*). Patch analyses used two to three secondary calibrations per clade, derived from the fossil-dated backbone. Patching of the 18 clades onto the backbone was undertaken using scripts modified from (*32*), resulting in an MCC dated phylogenetic tree of Annonaceae. We further merged 500 posterior trees (after a 20% burn-in) of each patch sequentially to the 500 backbone posterior backbone topologies to generate 500 posterior Annonaceae trees used for uncertainty evaluation.

Testing for rate heterogeneity

We used several complementary methods to test for diversification rate variation across our dated trees. Overall, we used ClaDS2 as the primary framework to assess lineage-specific diversification-rate heterogeneity, whereas BAMM and RPANDA were used to test for possible discrete diversification rate shifts and alternative diversification regimes. For all analyses and when possible, we accounted for unsampled species using a sampling fraction on a generic level (table S2). First, we inferred branch-specific diversification rates using ClaDS2 (*86*, *87*) from the PANDA package v0.8 in Julia. The ClaDS analysis was performed with 10,000 iterations in three independent chains. The chains converged, with a Gelman statistic of 1.00183. Second, we implemented BAMM [v2.5.0 (*88*)] to test for significant shifts in diversification rates. The Markov chain Monte Carlo (MCMC) was run for 80 million generations, sampling every 10,000 generations. BAMM convergence was checked in BAMMtools (*89*) using an initial 10% burn-in. MCMC convergence was assessed from log-likelihood traces and ESS values (>200). Event data were compared with a prior-only run to confirm that the results were not driven by the priors. We extracted the best shift configuration (expected four shifts) to identify the best supported rate-shift scenario and the most credible shift set (also expected four shifts) to visualize 99% credible configurations (fig. S2). Last, we tested whether diversification across the tree was correlated with a single homogeneous birth-death model, as expected under homogeneous diversification, or whether different parts of the tree were better fitted by distinct models, indicating heterogeneity in diversification dynamics (*90*). We used RPANDA shift estimates (*91*) to infer shifts in the modes of diversification. Shifts were estimated in a taxonomic approach based on tribes and subfamilies. We excluded the birth variable and death variable model

Downloaded from https://www.science.org on October 08, 2026

(BVAR_DVAR) because it showed unrealistic diversification rates, most likely an error based on the large size of the phylogeny. We calculated diversity dynamics with the probabilistic approach to identify the shift combinations based on the AICc values (fig. S4).

To address the issue of identifiability in estimating diversification from extant-only molecular phylogenies (*23*), we complemented our analyses with approaches based on PDR. These approaches avoid reliance on unidentifiable speciation and extinction parameters (*23*, *92*). We used the castor R package v1.8.7 (*93*) to compute pulled speciation rates (PSR), PDR, and deterministic LTT plots from the extant phylogeny using a maximum-likelihood framework. We used an age grid starting at 62 to 2 Ma to correct for potential biases, including limitations in deep time and the pull of the present (fig. S3). The increase and subsequent steep decline in PDR toward the present reflect known properties of topology-dependent calculations near the present (*23*, *92*).

The gamma (γ) statistic of (*94*) was calculated using the function gammaStat in APE (*95*) on the MCC tree and the 50 posterior trees. We found a significantly negative γ [−21.5*** ($P < 0.01$)], with posterior trees γ between −14 and −19 ($P < 0.01$), suggesting an early burst scenario (more branching events toward the bases of the trees). We also calculated the gamma statistic for five fully sampled extant time trees extracted from the augmented INSANE analysis (see below), as taxon sampling can have an impact on this statistic (*96*). The gamma statistic remained significantly negative (min: −20.63; max: −16.92; Supplementary Text).

Inferring diversity through time from the Cretaceous to the present

We inferred diversity through time using the fossil-informed birth-death diffusion framework of (*26*) using INSANE implemented in the Tapestree.jl program (https://ignacioq.github.io/Tapestree.jl/stable/). This method overcomes nonidentifiability issues by taking into account lineage heterogeneity based on topology and a birth-death diffusion model (*26*). By combining fossil-based extinction rate estimates, sampling fractions, and our near-complete phylogeny, this method allows inference of modeled complete phylogenies, including extinct, extant, and unsampled species. Extinction rates were estimated using PyRate v3.1.3-20230825 (*97*). PyRate uses the occurrences of fossils through time and calculates a fossil preservation rate based on a birth-death model, which, in turn, is used to estimate fossil-based speciation and extinction rates. Although Annonaceae have a relatively well-documented fossil record (*30*, *98*), we estimated extinction rates using the broader Magnoliales order, to which Annonaceae belongs (fig. S5, data S2, and Supplementary Text). Magnoliales is largely tropical and subtropical, and its other constituent families (e.g., Myristicaceae and Magnoliaceae) share similar life histories and ecological traits with Annonaceae. While we do not assume identical extinction dynamics across families, this approach provides a reasonable proxy for estimating extinction rate and substantially increases the number of fossil occurrences needed for improved modeling (Supplementary Materials and Methods). Epoch-constant rates (*45*) were estimated from 243 Magnoliales fossil occurrences with 124 assigned to Annonaceae (fig. S5 and table S4). Diversity-through-time plots were generated on the basis of 200 posterior sampled modeled complete phylogenies (Fig. 2) for the past 95 Myr (Fig. 3A). LTT plots were also generated from the 500 posterior extant trees as a comparison. We tested the sensitivity of our results by running INSANE with extinction rates from different fossil replicates and with posterior trees reflecting the oldest (101 Ma) and youngest (89 Ma) crown age estimates for Annonaceae.

Impact of mass extinction on extant phylogenetic tree

We tested for signals of mass extinction using the CoMET (Compound Poisson process on Mass-Extinction Times) model included in the R package TESS (*99*, *100*). The phylogeny was fitted under episodic birth-death models with two expected rate shifts and two mass extinction events. Survival probabilities from 5 to 50% in five percentage point intervals were modeled via beta priors. The MCMC runs estimated time-varying speciation and extinction rates, with significant shifts identified using posterior probabilities. We identified times where a mass extinction was strongly supported with a BF > 6 or showed decisive support with a BF > 10 following (*100*).

Correlates of diversification using environment-dependent birth-death models

We investigated which environmental factors are correlated with Annonaceae diversification by selecting 40 geographically located clades (referred to as geoclades), each concentrated in one of three major tropical regions (Asia-Pacific, South and Central America, and Africa, including Madagascar and the Mascarenes; Fig. 1 and table S5). Geoclades were defined as monophyletic lineages with at least 10 species and more than 75% of its distribution in a single region with a preference for clades containing more than 50 species (see data S3). These do not necessarily correspond to genera or tribes but represent regional lineages suitable for diversification analyses: Asia-Pacific (17 geoclades, representing 759 sampled species of 1020); Neotropics with subdivision into South and Central America including the Caribbean (12 geoclades, $^{745}/_{798}$ species); and Afrotropics including Madagascar (10 geoclades, $^{351}/_{357}$ species). In addition, one geoclade was restricted to southeast North America (genus *Asimina*, $^{11}/_{11}$ species). We tested a combination of region-specific and global environmental factors, selecting those most relevant to each tropical region (Supplementary Text and table S6). Global factors included sea level change and continental fragmentation, while regional factors included topography and paleotemperature following (*13*). For the latter, paleotemperature curves (fig. S10) were extracted for each region (fig. S13).

We tested environmental factors in a hypothesis-based approach (see Supplementary Text for the regional hypotheses and justification). We used birth-death environment-dependent models available in RPANDA v2.3 (*101*). We first fitted a constant-rate birth-death model as a null baseline, followed by fitting a set of time-dependent models (*102*) in which $\lambda(t)$ and $\mu(t)$ could vary through time. These time-dependent models were then used to initialize parameters for the environment-dependent models (table S6).

We selected a number of environmental variables relevant to biodiversity evolution in our regions of interest (fig. S10) rather than testing all possible predictors for every geoclade (table S5). First, three global scale variables were used: global temperature (*51*), sea level fluctuations (*103*), and continental fragmentation (*104*). Second, to take into account regional paleotemperature history, we used a recently published method to generate spatialized paleotemperature time series for the past 100 Myr (*13*). Here, we focused on our four regions defined above (fig. S10) following (*13*). These regions consider plate tectonics and changing configurations over the past 100 Myr and are relevant to the evolution of tropical climates. Last, for South American geoclades, we tested Andean uplift using the paleoelevation curves from (*105*) (tables S5 and S6). To assess sensitivity to dating uncertainty, all analyses were repeated across 50 randomly selected posterior trees (data S3).

Downloaded from https://www.science.org on October 08, 2026

Model fit was evaluated with AICc, comparing null, time-, and environment-dependent models. Delta AICc and Akaike weights (ωAIC) were used to identify the best-fitting models per clade; only the top three models with ωAIC > 0.1 were retained. For posterior trees, only the best model per tree was kept, and frequencies of model categories were calculated (data S3). Model fit showed no significant association with geoclade properties (fig. S11), except that clades correlated with sea level variation had younger crown ages.

Because time-continuous birth-death models can suffer from identifiability limitations when inferring speciation and extinction rates from extant-only phylogenies (*23*), we validated the best-fitting environmental-dependent model identified in RPANDA using a Bayesian approach implemented in RevBayes (*106*). Diversification was modeled using episodic birth-death models with up to 100 intervals (reduced where predictors had fewer data points), in which rates are constant within discrete time intervals but allowed to vary between intervals. Environmental dependence was incorporated by linking rate variation to the predictor identified in the RPANDA analysis. Sampling fractions were included. Two MCMC chains of ≥50,000 generations were run, extended up to 500,000 generations, and reduced intervals (≥50) if convergence was not achieved. Convergence was assessed via ESS (>200) and trace plots (data S3). Model support was classified into four categories: (i) supported ("s"), when RevBayes results were consistent with the RPANDA-inferred model; (ii) not supported—disagree (*)—when RevBayes favored an alternative model; (iii) inconclusive ("i"), when no clear distinction among models could be made; and (iv) not converging ("nc"), when RevBayes analyses did not converge.

Supplementary Materials

The PDF file includes:

Supplementary Text
Figs. S1 to S13
Tables S1 to S6
Legends for data S1 to S3
References

Other Supplementary Material for this manuscript includes the following:

Data S1 to S3

REFERENCES

1. W. L. Eiserhardt, T. L. P. Couvreur, W. J. Baker, Plant phylogeny as a window on the evolution of hyperdiversity in the tropical rainforest biome. *New Phytol.* **214**, 1408–1422 (2017).
2. R. J. Morley, *Origin and Evolution of Tropical Rain Forests* (John Wiley & Sons, 2000).
3. J. E. Richardson, R. T. Pennington, T. D. Pennington, P. M. Hollingsworth, Rapid diversification of a species-rich genus of neotropical rain forest trees. *Science* **293**, 2242–2245 (2001).
4. C. C. Davis, C. O. Webb, K. J. Wurdack, C. A. Jaramillo, M. J. Donoghue, Explosive radiation of Malpighiales supports a mid-Cretaceous origin of modern tropical rain forests. *Am. Nat.* **165**, E36–E65 (2005).
5. R. H. J. Erkens, L. W. Chatrou, J. W. Maas, T. van der Niet, V. Savolainen, A rapid diversification of rainforest trees (*Guatteria*; Annonaceae) following dispersal from Central into South America. *Mol. Phylogenet. Evol.* **44**, 399–411 (2007).
6. E. J. M. Koenen, J. J. Clarkson, T. D. Pennington, L. W. Chatrou, Recently evolved diversity and convergent radiations of rainforest mahoganies (Meliaceae) shed new light on the origins of rainforest hyperdiversity. *New Phytol.* **207**, 327–339 (2015).
7. A. Gamisch, H. P. Comes, Clade-age-dependent diversification under high species turnover shapes species richness disparities among tropical rainforest lineages of *Bulbophyllum* (Orchidaceae). *BMC Evol. Biol.* **19**, 93 (2019).
8. W. Li, R. Wang, M.-F. Liu, R. A. Folk, B. Xue, R. M. K. Saunders, Climatic and biogeographic processes underlying the diversification of the pantropical flowering plant family Annonaceae. *Front. Plant Sci.* **15**, 1287171 (2024).
9. A. Antonelli, A. Zizka, D. Silvestro, R. Scharn, B. Cascales-Miñana, C. D. Bacon, An engine for global plant diversity: Highest evolutionary turnover and emigration in the American tropics. *Front. Genet.* **6**, 130 (2015).
10. O. Hagen, A. Skeels, R. E. Onstein, W. Jetz, L. Pellissier, Earth history events shaped the evolution of uneven biodiversity across tropical moist forests. *Proc. Natl. Acad. Sci. U.S.A.* **118**, e2026347118 (2021).
11. A. S. Meseguer, A. Michel, P.-H. Fabre, O. A. Pérez Escobar, G. Chomicki, R. Riina, A. Antonelli, P.-O. Antoine, F. Delsuc, F. L. Condamine, Diversification dynamics in the Neotropics through time, clades, and biogeographic regions. *eLife* **11**, e74503 (2022).
12. M. Tietje, A. Antonelli, W. J. Baker, R. Govaerts, S. A. Smith, W. L. Eiserhardt, Global variation in diversification rate and species richness are unlinked in plants. *Proc. Natl. Acad. Sci. U.S.A.* **119**, e2120662119 (2022).
13. D. Tardif, F. L. Condamine, S. J. R. Streiff, P. Sepulchre, T. L. P. Couvreur, Generating spatialised and seasonal deep-time palaeoclimatic information: Integration Into an environmental-dependent diversification model. *Glob. Ecol. Biogeogr.* **34**, e70024 (2025).
14. C. Hoorn, F. P. Wesselingh, H. Ter Steege, M. A. Bermudez, A. Mora, J. Sevink, I. Sanmartín, A. Sanchez-Meseguer, C. L. Anderson, J. P. Figueiredo, C. Jaramillo, D. Riff, F. R. Negri, H. Hooghiemstra, J. Lundberg, T. Stadler, T. Särkinen, A. Antonelli, Amazonia through time: Andean uplift, climate change, landscape evolution, and biodiversity. *Science* **330**, 927–931 (2010).
15. D. Moen, H. Morlon, Why does diversification slow down? *Trends Ecol. Evol.* **29**, 190–197 (2014).
16. C. H. Graham, D. Storch, A. Machac, Phylogenetic scale in ecology and evolution. *Glob. Ecol. Biogeogr.* **27**, 175–187 (2018).
17. T. L. P. Couvreur, G. Dauby, A. Blach-Overgaard, V. Deblauwe, S. Dessein, V. Droissart, O. J. Hardy, D. J. Harris, S. B. Janssens, A. C. Ley, B. A. Mackinder, B. Sonké, M. S. M. Sosef, T. Stévart, J.-C. Svenning, J. J. Wieringa, A. Faye, A. D. Missoup, K. A. Tolley, V. Nicolas, S. Ntie, F. Fluteau, C. Robin, F. Guillocheau, D. Barboni, P. Sepulchre, Tectonics, climate and the diversification of the tropical African terrestrial flora and fauna. *Biol. Rev.* **96**, 16–51 (2021).
18. M. R. Carvalho, C. Jaramillo, F. de la Parra, D. Caballero-Rodríguez, F. Herrera, S. Wing, B. L. Turner, C. D'Apolito, M. Romero-Báez, P. Narváez, C. Martínez, M. Gutierrez, C. Labandeira, G. Bayona, M. Rueda, M. Paez-Reyes, D. Cárdenas, Á. Duque, J. L. Crowley, C. Santos, D. Silvestro, Extinction at the end-Cretaceous and the origin of modern Neotropical rainforests. *Science* **372**, 63–68 (2021).
19. M. J. Benton, P. Wilf, H. Sauquet, The Angiosperm Terrestrial Revolution and the origins of modern biodiversity. *New Phytol.* **233**, 2017–2035 (2022).
20. S. Ramírez-Barahona, H. Sauquet, S. Magallón, The delayed and geographically heterogeneous diversification of flowering plant families. *Nat. Ecol. Evol.* **4**, 1232–1238 (2020).
21. A. R. Zuntini, T. Carruthers, O. Maurin, P. C. Bailey, K. Leempoel, G. E. Brewer, N. Epitawalage, E. Françoso, B. Gallego-Paramo, C. McGinnie, R. Negrão, S. R. Roy, L. Simpson, E. T. Romero, V. M. A. Barber, L. Botigué, J. J. Clarkson, R. S. Cowan, S. Dodsworth, M. G. Johnson, J. T. Kim, L. Pokorny, N. J. Wickett, G. M. Antar, L. DeBolt, K. Gutierrez, K. P. Hendriks, A. Hoewener, A.-Q. Hu, E. M. Joyce, I. A. B. S. Kikuchi, I. Larridon, D. A. Larson, E. J. de Lírio, J.-X. Liu, P. Malakasi, N. A. S. Przelomska, T. Shah, J. Viruel, T. R. Allnutt, G. K. Ameka, R. L. Andrew, M. S. Appelhans, M. Arista, M. J. Ariza, J. Arroyo, W. Arthan, J. B. Bachelier, C. D. Bailey, H. F. Barnes, M. D. Barrett, R. L. Barrett, R. J. Bayer, M. J. Bayly, E. Biffin, N. Biggs, J. L. Birch, D. Bogarín, R. Borosova, A. M. C. Bowles, P. C. Boyce, G. L. C. Bramley, M. Briggs, L. Broadhurst, G. K. Brown, J. J. Bruhl, A. Bruneau, S. Buerki, E. Burns, M. Byrne, S. Cable, A. Calladine, M. W. Callmander, Á. Cano, D. J. Cantrill, W. M. Cardinal-McTeague, M. M. Carlsen, A. J. A. Carruthers, A. de Castro Mateo, M. W. Chase, L. W. Chatrou, M. Cheek, S. Chen, M. J. M. Christenhusz, P.-A. Christin, M. A. Clements, S. C. Coffey, J. G. Conran, X. Cornejo, T. L. P. Couvreur, I. D. Cowie, L. Csiba, I. Darbyshire, G. Davidse, N. M. J. Davies, A. P. Davis, K. van Dijk, S. R. Downie, M. F. Duretto, M. R. Duvall, S. L. Edwards, U. Eggli, R. H. J. Erkens, M. Escudero, M. de la Estrella, F. Fabriani, M. F. Fay, P. d. L. Ferreira, S. Z. Ficinski, R. M. Fowler, S. Frisby, L. Fu, T. Fulcher, M. Galbany-Casals, E. M. Gardner, D. A. German, A. Giaretta, M. Gibernau, L. J. Gillespie, C. C. González, D. J. Goyder, S. W. Graham, A. Grall, L. Green, B. F. Gunn, D. G. Gutiérrez, J. Hackel, T. Haevermans, A. Haigh, J. C. Hall, T. Hall, M. J. Harrison, S. A. Hatt, O. Hidalgo, T. R. Hodkinson, G. D. Holmes, H. C. F. Hopkins, C. J. Jackson, S. A. James, R. W. Jobson, G. Kadereit, I. M. Kahandawala, K. Kainulainen, M. Kato, E. A. Kellogg, G. J. King, B. Klejevskaja, B. B. Klitgaard, R. R. Klopper, S. Knapp, M. A. Koch, J. H. Leebens-Mack, F. Lens, C. J. Leon, É. Léveillé-Bourret, G. P. Lewis, D.-Z. Li, L. Li, S. Liede-Schumann, T. Livshultz, D. Lorence, M. Lu, P. Lu-Irving, J. Luber, E. J. Lucas, M. Luján, M. Lum, T. D. Macfarlane, C. Magdalena, V. F. Mansano, L. E. Masters, S. J. Mayo, K. McColl, A. J. McDonnell, A. E. McDougall, T. G. B. McLay, H. McPherson, R. I. Meneses, V. S. F. T. Merckx, F. A. Michelangeli, J. D. Mitchell, A. K. Monro, M. J. Moore, T. L. Mueller, K. Mummenhoff, J. Munzinger, P. Muriel, D. J. Murphy, K. Nargar, L. Nauheimer, F. J. Nge, R. Nyffeler, A. Orejuela, E. M. Ortiz, L. Palazzesi, A. L. Peixoto, S. K. Pell, J. Pellicer, D. S. Penneys, O. A. Perez-Escobar, C. Persson, M. Pignal, Y. Pillon, J. R. Pirani, G. M. Plunkett, R. F. Powell, G. T. Prance, C. Puglisi, M. Qin, R. K. Rabeler, P. E. J. Rees, M. Renner, E. H. Roalson, M. Rodda, Z. S. Rogers, S. Rokni, R. Rutishauser, M. F. de Salas,

Downloaded from https://www.science.org on October 08, 2026

H. Schaefer, R. J. Schley, A. Schmidt-Lebuhn, A. Shapcott, I. Al-Shehbaz, K. A. Shepherd, M. P. Simmons, A. O. Simões, A. R. G. Simões, M. Siros, E. C. Smidt, J. F. Smith, N. Snow, D. E. Soltis, P. S. Soltis, R. J. Soreng, C. A. Sothers, J. R. Starr, P. F. Stevens, S. C. K. Straub, L. Struwe, J. M. Taylor, I. R. H. Telford, A. H. Thornhill, I. Tooth, A. Trias-Blasi, F. Udovicic, T. M. A. Utteridge, J. C. Del Valle, G. A. Verboom, H. P. Vonow, M. S. Vorontsova, J. M. de Vos, N. Al-Wattar, M. Waycott, C. A. D. Welker, A. J. White, J. J. Wieringa, L. T. Williamson, T. C. Wilson, S. Y. Wong, L. A. Woods, R. Woods, S. Worboys, M. Xanthos, Y. Yang, Y.-X. Zhang, M.-Y. Zhou, S. Zmarzty, F. O. Zuloaga, A. Antonelli, S. Bellot, D. M. Crayn, O. M. Grace, P. J. Kersey, I. J. Leitch, H. Sauquet, S. A. Smith, W. L. Eiserhardt, F. Forest, W. J. Baker, Phylogenomics and the rise of the angiosperms. *Nature* **629**, 843–850 (2024).
22. C. Coiffard, H. El Atfy, J. Renaudie, R. Bussert, D. Uhl, The emergence of the tropical rainforest biome in the Cretaceous. *Biogeosciences* **20**, 1145–1154 (2023).
23. S. Louca, M. W. Pennell, Extant timetrees are consistent with a myriad of diversification histories. *Nature* **580**, 502–505 (2020).
24. T. B. Quental, C. R. Marshall, Diversity dynamics: Molecular phylogenies need the fossil record. *Trends Ecol. Evol.* **25**, 434–441 (2010).
25. H. Morlon, J. Andréoletti, J. Barido-Sottani, S. Lambert, B. Perez-Lamarque, I. Quintero, V. Senderov, P. Veron, Phylogenetic insights into diversification. *Annu. Rev. Ecol. Evol. Syst.* **55**, 1–21 (2024).
26. I. Quintero, N. Lartillot, H. Morlon, Imbalanced speciation pulses sustain the radiation of mammals. *Science* **384**, 1007–1012 (2024).
27. F. J. Nge, T. Chaowasku, A. Damthongdee, C. Wiya, V. R. C. Soulé, C. Rodrigues-Vaz, D. Bruy, C. Mariac, L. W. Chatrou, J. Chen, L. M. Choo, L.-P. M. J. Dagallier, R. H. J. Erkens, D. M. Johnson, C. Leeratiwong, A. Q. Lobão, J. C. Lopes, M. F. Martínez-Velarde, J. Munzinger, N. A. Murray, W. L. Neo, M. Rakotoarinivo, A. E. Ortiz-Rodriguez, B. Sonké, D. C. Thomas, J. J. Wieringa, T. L. P. Couvreur, Complete genus-level phylogenomics and new subtribal classification of the pantropical plant family Annonaceae. *TAXON* **73**, 1341–1369 (2024).
28. R. H. J. Erkens, L. M. P. Blanpain, I. C. Jara, K. Runge, N. Verspagen, A. Cosiaux, T. L. P. Couvreur, Spatial distribution of Annonaceae across biomes and anthromes: Knowledge gaps in spatial and ecological data. *Plants People Planet* **5**, 520–535 (2023).
29. S. W. Punyasena, G. Eshel, J. C. McElwain, The influence of climate on the spatial patterning of Neotropical plant families. *J. Biogeogr.* **35**, 117–130 (2008).
30. M. D. Pirie, J. A. Doyle, Dating clades with fossils and molecules: The case of Annonaceae. *Bot. J. Linn. Soc.* **169**, 84–116 (2012).
31. J. Massoni, T. L. P. Couvreur, H. Sauquet, Five major shifts of diversification through the long evolutionary history of Magnoliidae (angiosperms). *BMC Evol. Biol.* **15**, 49 (2015).
32. N. S. Upham, J. A. Esselstyn, W. Jetz, Inferring the mammal tree: Species-level sets of phylogenies for questions in ecology, evolution, and conservation. *PLoS Biol.* **17**, e3000494 (2019).
33. M. Takahashi, E. M. Friis, K. Uesugi, Y. Suzuki, P. R. Crane, Floral evidence of Annonaceae from the Late Cretaceous of Japan. *Int. J. Plant Sci.* **169**, 908–917 (2008).
34. M. G. Harvey, G. A. Bravo, S. Claramunt, A. M. Cuervo, G. E. Derryberry, J. Battilana, G. F. Seeholzer, J. S. McKay, B. C. O'Meara, B. C. Faircloth, S. V. Edwards, J. Pérez-Emán, R. G. Moyle, F. H. Sheldon, A. Aleixo, B. T. Smith, R. T. Chesser, L. F. Silveira, J. Cracraft, R. T. Brumfield, E. P. Derryberry, The evolution of a tropical biodiversity hotspot. *Science* **370**, 1343–1348 (2020).
35. B. C. O'Meara, J. M. Beaulieu, Noise leads to the perceived increase in evolutionary rates over short time scales. *PLoS Comput. Biol.* **20**, e1012458 (2024).
36. W. J. Baker, T. L. P. Couvreur, Global biogeography and diversification of palms sheds light on the evolution of tropical lineages. II. Diversification history and origin of regional assemblages. *J. Biogeogr.* **40**, 286–298 (2013).
37. Á. Cano, F. W. Stauffer, T. Andermann, I. M. Liberal, A. Zizka, C. D. Bacon, H. Lorenzi, C. Christe, M. Töpel, M. Perret, A. Antonelli, Recent and local diversification of Central American understorey palms. *Glob. Ecol. Biogeogr.* **31**, 1513–1525 (2022).
38. L.-P. M. J. Dagallier, F. L. Condamine, T. L. P. Couvreur, Sequential diversification with Miocene extinction and Pliocene speciation linked to mountain uplift explains the diversity of the African rain forest clade Monodoreae (Annonaceae). *Ann. Bot.* **133**, 677–696 (2024).
39. T. J. Givnish, Adaptive radiation versus 'radiation' and 'explosive diversification': Why conceptual distinctions are fundamental to understanding evolution. *New Phytol.* **207**, 297–303 (2015).
40. B. Xue, X. Guo, J. B. Landis, M. Sun, C. C. Tang, P. S. Soltis, D. E. Soltis, R. M. K. Saunders, Accelerated diversification correlated with functional traits shapes extant diversity of the early divergent angiosperm family Annonaceae. *Mol. Phylogenet. Evol.* **142**, 106659 (2020).
41. R. M. Kooyman, R. J. Morley, D. M. Crayn, E. M. Joyce, M. Rossetto, J. W. F. Slik, J. S. Strijk, T. Su, J.-Y. S. Yap, P. Wilf, Origins and assembly of Malesian rainforests. *Annu. Rev. Ecol. Evol. Syst.* **50**, 119–143 (2019).
42. W. Wang, R. D. C. Ortiz, F. M. B. Jacques, X.-G. Xiang, H.-L. Li, L. Lin, R.-Q. Li, Y. Liu, P. S. Soltis, D. E. Soltis, Z.-D. Chen, Menispermaceae and the diversification of tropical rainforests near the Cretaceous–Paleogene boundary. *New Phytol.* **195**, 470–478 (2012).
43. T. L. P. Couvreur, F. Forest, W. J. Baker, Origin and global diversification patterns of tropical rain forests: Inferences from a complete genus-level phylogeny of palms. *BMC Biol.* **9**, 44 (2011).
44. C. Jaramillo, M. J. Rueda, G. Mora, Cenozoic plant diversity in the Neotropics. *Science* **311**, 1893–1896 (2006).
45. D. Silvestro, B. Cascales-Miñana, C. D. Bacon, A. Antonelli, Revisiting the origin and diversification of vascular plants through a comprehensive Bayesian analysis of the fossil record. *New Phytol.* **207**, 425–436 (2015).
46. R. J. Morley, "Cretaceous and tertiary climate change and the past distribution of megathermal rainforests," in *Tropical Rainforest Responses to Climatic Changes*, M. B. Bush, J. Flenley, Eds. (Praxis Publishing, 2007), pp. 1–31.
47. J. B. Thompson, S. Ramírez-Barahona, No phylogenetic evidence for angiosperm mass extinction at the Cretaceous–Palaeogene (K-Pg) boundary. *Biol. Lett.* **19**, 20230314 (2023).
48. P. Wilf, M. R. Carvalho, E. Stiles, The end-Cretaceous plant extinction: Heterogeneity, ecosystem transformation, and insights for the future. *Camb. Prisms Extinct.* **1**, e14 (2023).
49. C. Jaramillo, D. Ochoa, L. Contreras, M. Pagani, H. Carvajal-Ortiz, L. M. Pratt, S. Krishnan, A. Cardona, M. Romero, L. Quiroz, G. Rodriguez, M. J. Rueda, F. de la Parra, S. Morón, W. Green, G. Bayona, C. Montes, O. Quintero, R. Ramirez, G. Mora, S. Schouten, H. Bermudez, R. Navarrete, F. Parra, M. Alvarán, J. Osorno, J. L. Crowley, V. Valencia, J. Vervoort, Effects of rapid global warming at the Paleocene-Eocene boundary on neotropical vegetation. *Science* **330**, 957–961 (2010).
50. C. Hoorn, L. G. Lohmann, L. M. Boschman, F. L. Condamine, Neogene history of the Amazonian flora: A perspective based on geological, palynological, and molecular phylogenetic data. *Annu. Rev. Earth Planet. Sci.* **51**, 419–446 (2023).
51. T. Westerhold, N. Marwan, A. J. Drury, D. Liebrand, C. Agnini, E. Anagnostou, J. S. K. Barnet, S. M. Bohaty, D. De Vleeschouwer, F. Florindo, T. Frederichs, D. A. Hodell, A. E. Holbourn, D. Kroon, V. Lauretano, K. Littler, L. J. Lourens, M. Lyle, H. Pälike, U. Röhl, J. Tian, R. H. Wilkens, P. A. Wilson, J. C. Zachos, An astronomically dated record of Earth's climate and its predictability over the last 66 million years. *Science* **369**, 1383–1387 (2020).
52. F. L. Condamine, J. Rolland, H. Morlon, Assessing the causes of diversification slowdowns: Temperature-dependent and diversity-dependent models receive equivalent support. *Ecol. Lett.* **22**, 1900–1912 (2019).
53. R. H. MacArthur, E. O. Wilson, *The Theory of Island Biogeography* (Princeton Univ. Press, 1967).
54. M. de Bruyn, L. Rüber, S. Nylinder, B. Stelbrink, N. R. Lovejoy, S. Lavoué, H. H. Tan, E. Nugroho, D. Wowor, P. K. L. Ng, M. N. Siti Azizah, T. Von Rintelen, R. Hall, G. R. Carvalho, Paleo-drainage basin connectivity predicts evolutionary relationships across three Southeast Asian biodiversity hotspots. *Syst. Biol.* **62**, 398–410 (2013).
55. B. G. Kuhnhäuser, C. D. Bates, J. Dransfield, C. Geri, A. Henderson, S. Julia, J. Y. Lim, R. J. Morley, H. Rustiami, R. J. Schley, S. Bellot, G. Chomicki, W. L. Eiserhardt, S. J. Hiscock, W. J. Baker, Island geography drives evolution of rattan palms in tropical Asian rainforests. *Science* **387**, 1204–1209 (2025).
56. M. D. Pirie, P. J. M. Maas, R. A. Wilschut, H. Melchers-Sharrott, L. W. Chatrou, Parallel diversifications of Cremastosperma and Mosannona (Annonaceae), tropical rainforest trees tracking Neogene upheaval of South America. *R. Soc. Open Sci.* **5**, 171561 (2018).
57. C. D. Bacon, D. Silvestro, C. Jaramillo, B. T. Smith, P. Chakrabarty, A. Antonelli, Biological evidence supports an early and complex emergence of the Isthmus of Panama. *Proc. Natl. Acad. Sci. U.S.A.* **112**, 6110–6115 (2015).
58. R. J. Morley, The establishment of Palaeotropical rainforests from Africa to Oceania in relation to plate tectonics and zonal tropical climates. *Geol. Soc. Spec. Publ.* **549**, 113–136 (2025).
59. M. Bansal, R. J. Morley, S. K. Nagaraju, S. Dutta, A. K. Mishra, J. Selveraj, S. Kumar, D. Niyolia, S. M. Harish, O. B. Abdelrahim, S. E. Hasan, B. R. Ramesh, S. Dayanandan, H. P. Morley, P. S. Ashton, V. Prasad, Southeast Asian Dipterocarp origin and diversification driven by Africa-India floristic interchange. *Science* **375**, 455–460 (2022).
60. X. Delclòs, E. Peñalver, C. Jaramillo, E. Cadena, C. Menor-Salván, J. L. Román, R. F. Castaño-Cardona, D. Peris, M. Carvalho, D. Quiroz-Cabascango, M. R. Carvalho, P. Blomenkemper, F. Herrera, P. Santamarina, M. Santer, G. Carrera, M. M. Solórzano-Kraemer, Cretaceous amber of Ecuador unveils new insights into South America's Gondwanan forests. *Commun. Earth Environ.* **6**, 745 (2025).
61. W. Ding, D. Silvestro, R. E. Onstein, M. Wu, Z. Zhou, Y. Xing, The stepwise rise of angiosperm-dominated terrestrial ecosystems. *Biol. Rev.* **100**, 2131–2149 (2025).
62. T. S. Feild, T. J. Brodribb, A. Iglesias, D. S. Chatelet, A. Baresch, G. R. Upchurch, B. Gomez, B. A. R. Mohr, C. Coiffard, J. Kvacek, C. Jaramillo, Fossil evidence for Cretaceous escalation in angiosperm leaf vein evolution. *Proc. Natl. Acad. Sci. U.S.A.* **108**, 8363–8366 (2011).
63. A. B. Leslie, C. Simpson, L. Mander, Reproductive innovations and pulsed rise in plant complexity. *Science* **373**, 1368–1372 (2021).
64. D. Peris, F. L. Condamine, The angiosperm radiation played a dual role in the diversification of insects and insect pollinators. *Nat. Commun.* **15**, 552 (2024).
65. C. K. Boyce, T. J. Brodribb, T. S. Feild, M. A. Zwieniecki, Angiosperm leaf vein evolution was physiologically and environmentally transformative. *Proc. R. Soc. B Biol. Sci.* **276**, 1771–1776 (2009).

Downloaded from https://www.science.org on October 08, 2026

66. D. Silvestro, M. F. Tejedor, M. L. Serrano-Serrano, O. Loiseau, V. Rossier, J. Rolland, A. Zizka, S. Höhna, A. Antonelli, N. Salamin, Early arrival and climatically-linked geographic expansion of New World monkeys from tiny African ancestors. *Syst. Biol.* **68**, 78–92 (2019).
67. C. C. Davis, The herbarium of the future. *Trends Ecol. Evol.* **38**, 412–423 (2023).
68. J. M. Heberling, J. T. Miller, D. Noesgaard, S. B. Weingart, D. Schigel, Data integration enables global biodiversity synthesis. *Proc. Natl. Acad. Sci. U.S.A.* **118**, e2018093118 (2021).
69. C. C. Davis, E. Sessa, A. Paton, A. Antonelli, J. K. Teisher, Guidelines for the effective and ethical sampling of herbaria. *Nat. Ecol. Evol.* **9**, 196–203 (2025).
70. T. L. P. Couvreur, A. J. Helmstetter, E. J. M. Koenen, K. Bethune, R. D. Brandão, S. A. Little, H. Sauquet, R. H. J. Erkens, Phylogenomics of the major tropical plant family Annonaceae using targeted enrichment of nuclear genes. *Front. Plant Sci.* **9**, 1941 (2019).
71. V. R. C. Soulé, T. L. P. Couvreur, C. Mariac, "Annonaceae DNA extraction protocol from silicagel dried and herbarium preserved leaves" (protocols.io, 2023); doi:10.17504/protocols.io.5qpvorqx9v4o/v1.
72. V. R. C. Soulé, C. Mariac, T. Delaigue, T. L. P. Couvreur, "Illumina library preparation and dual hybridization protocol of ERC GLOBAL V.3" (protocols.io, 2024); doi:10.17504/protocols.io.n92ldp787l5b/v3.
73. M. G. Johnson, E. M. Gardner, Y. Liu, R. Medina, B. Goffinet, A. J. Shaw, N. J. C. Zerega, N. J. Wickett, HybPiper: Extracting coding sequence and introns for phylogenetics from high-throughput sequencing reads using target enrichment. *Appl. Plant Sci.* **4**, 1600016 (2016).
74. Z. Q. Shee, D. G. Frodin, R. Cámara-Leret, L. Pokorny, Reconstructing the complex evolutionary history of the Papuasian *Schefflera* radiation through herbariomics. *Front. Plant Sci.* **11**, 258 (2020).
75. S. Álvarez-Carretero, A. U. Tamuri, M. Battini, F. F. Nascimento, E. Carlisle, R. J. Asher, Z. Yang, P. C. J. Donoghue, M. D. Reis, A species-level timeline of mammal evolution integrating phylogenomic data. *Nature* **602**, 263–267 (2022).
76. A. J. Helmstetter, Z. Ezedin, E. J. de Lírio, S. M. de Oliveira, L. W. Chatrou, R. H. J. Erkens, I. Larridon, K. Leempoel, O. Maurin, S. Roy, A. R. Zuntini, W. J. Baker, T. L. P. Couvreur, F. Forest, H. Sauquet, Toward a phylogenomic classification of magnoliids. *Am. J. Bot.* **112**, e16451 (2025).
77. M. G. Johnson, L. Pokorny, S. Dodsworth, L. R. Botigué, R. S. Cowan, A. Devault, W. L. Eiserhardt, N. Epitawalage, F. Forest, J. T. Kim, J. H. Leebens-Mack, I. J. Leitch, O. Maurin, D. E. Soltis, P. S. Soltis, G. Ka-Shu Wong, W. J. Baker, N. J. Wickett, A universal probe set for targeted sequencing of 353 nuclear genes from any flowering plant designed using k-medoids clustering. *Syst. Biol.* **68**, 594–606 (2019).
78. J. Massoni, J. Doyle, H. Sauquet, Fossil calibration of Magnoliidae, an ancient lineage of angiosperms. *Palaeontol. Electron.* **18**, 1–25 (2015).
79. A. Stamatakis, RAxML version 8: A tool for phylogenetic analysis and post-analysis of large phylogenies. *Bioinformatics* **30**, 1312–1313 (2014).
80. C. Zhang, E. Sayyari, S. Mirarab, "ASTRAL-III: Increased scalability and impacts of contracting low-support branches," in *Comparative Genomics: 15th International Workshop, RECOMB-CG 2017*, J. Meidanis, L. Nakhleh, Eds., *Lecture Notes in Computer Science 10562* (Springer International Publishing, 2017), pp. 53–75.
81. S. A. Smith, B. C. O'Meara, treePL: Divergence time estimation using penalized likelihood for large phylogenies. *Bioinformatics* **28**, 2689–2690 (2012).
82. S. A. Smith, J. W. Brown, J. F. Walker, So many genes, so little time: A practical approach to divergence-time estimation in the genomic era. *PLOS ONE* **13**, e0197433 (2018).
83. R. Bouckaert, T. G. Vaughan, J. Barido-Sottani, S. Duchêne, M. Fourment, A. Gavryushkina, J. Heled, G. Jones, D. Kühnert, N. D. Maio, M. Matschiner, F. K. Mendes, N. F. Müller, H. A. Ogilvie, L. du Plessis, A. Popinga, A. Rambaut, D. Rasmussen, I. Siveroni, M. A. Suchard, C.-H. Wu, D. Xie, C. Zhang, T. Stadler, A. J. Drummond, BEAST 2.5: An advanced software platform for Bayesian evolutionary analysis. *PLoS Comput. Biol.* **15**, e1006650 (2019).
84. M. A. Miller, W. Pfeiffer, T. Schwartz, "The CIPRES Science Gateway: A community resource for phylogenetic analyses," in *Proceedings of the 2011 TeraGrid Conference: Extreme Digital Discovery* (ACM, New York, 2011), article 41, pp. 1–8.
85. A. Rambaut, M. A. Suchard, D. Xie, A. J. Drummond, Tracer v1.6 (2014); http://tree.bio.ed.ac.uk/software/tracer/.
86. O. Maliet, F. Hartig, H. Morlon, A model with many small shifts for estimating species-specific diversification rates. *Nat. Ecol. Evol.* **3**, 1086–1092 (2019).
87. O. Maliet, H. Morlon, Fast and accurate estimation of species-specific diversification rates using data augmentation. *Syst. Biol.* **71**, 353–366 (2022).
88. D. L. Rabosky, Automatic detection of key innovations, rate shifts, and diversity-dependence on phylogenetic trees. *PLOS ONE* **9**, e89543 (2014).
89. D. L. Rabosky, M. Grundler, C. Anderson, P. Title, J. J. Shi, J. W. Brown, H. Huang, J. G. Larson, BAMMtools: An R package for the analysis of evolutionary dynamics on phylogenetic trees. *Methods Ecol. Evol.* **5**, 701–707 (2014).
90. H. Morlon, T. L. Parsons, J. B. Plotkin, Reconciling molecular phylogenies with the fossil record. *Proc. Natl. Acad. Sci. U.S.A.* **108**, 16327–16332 (2011).
91. N. Mazet, H. Morlon, P.-H. Fabre, F. L. Condamine, Estimating clade-specific diversification rates and palaeodiversity dynamics from reconstructed phylogenies. *Methods Ecol. Evol.* **14**, 2575–2591 (2023).
92. A. J. Helmstetter, S. Glemin, J. Käfer, R. Zenil-Ferguson, H. Sauquet, H. de Boer, L.-P. M. J. Dagallier, N. Mazet, E. L. Reboud, T. L. P. Couvreur, F. L. Condamine, Pulled diversification rates, lineages-through-time plots, and modern macroevolutionary modeling. *Syst. Biol.* **71**, 758–773 (2022).
93. S. Louca, M. Doebeli, Efficient comparative phylogenetics on large trees. *Bioinformatics* **34**, 1053–1055 (2018).
94. O. G. Pybus, P. H. Harvey, Testing macro-evolutionary models using incomplete molecular phylogenies. *Proc. R. Soc. B Biol. Sci.* **267**, 2267–2272 (2000).
95. A.-A. Popescu, K. T. Huber, E. Paradis, ape 3.0: New tools for distance-based phylogenetics and evolutionary analysis in R. *Bioinformatics* **28**, 1536–1537 (2012).
96. J. A. Fordyce, Interpreting the γ statistic in phylogenetic diversification rate studies: A rate decrease does not necessarily indicate an early burst. *PLOS ONE* **5**, e11781 (2010).
97. D. Silvestro, N. Salamin, J. Schnitzler, PyRate: A new program to estimate speciation and extinction rates from incomplete fossil data. *Methods Ecol. Evol.* **5**, 1126–1131 (2014).
98. Q. Li, G. Shi, Y. Liu, Q. Fu, J. Jin, C. Quan, The early history of Annonaceae (Magnoliales) in Southeast Asia suggests floristic exchange between India and Pan-Indochina by the late Oligocene. *Pap. Palaeontol.* **5**, 601–612 (2019).
99. S. Höhna, M. R. May, B. R. Moore, TESS: An R package for efficiently simulating phylogenetic trees and performing Bayesian inference of lineage diversification rates. *Bioinformatics* **32**, 789–791 (2016).
100. M. R. May, S. Höhna, B. R. Moore, A Bayesian approach for detecting the impact of mass-extinction events on molecular phylogenies when rates of lineage diversification may vary. *Methods Ecol. Evol.* **7**, 947–959 (2016).
101. F. L. Condamine, J. Rolland, H. Morlon, Macroevolutionary perspectives to environmental change. *Ecol. Lett.* **16**, 72–85 (2013).
102. H. Morlon, D. W. Schwilk, J. A. Bryant, P. A. Marquet, A. G. Rebelo, C. Tauss, B. J. M. Bohannan, J. L. Green, Spatial patterns of phylogenetic diversity. *Ecol. Lett.* **14**, 141–149 (2011).
103. K. G. Miller, J. V. Browning, W. J. Schmelz, R. E. Kopp, G. S. Mountain, J. D. Wright, Cenozoic sea level and cryospheric evolution from deep-sea geochemical and continental margin records. *Sci. Adv.* **6**, eaaz1346 (2020).
104. A. Zaffos, S. Finnegan, S. E. Peters, Plate tectonic regulation of global marine animal diversity. *Proc. Natl. Acad. Sci. U.S.A.* **114**, 5653–5658 (2017).
105. L. M. Boschman, F. L. Condamine, Mountain radiations are not only rapid and recent: Ancient diversification of South American frog and lizard families related to Paleogene Andean orogeny and Cenozoic climate variations. *Glob. Planet. Change* **208**, 103704 (2022).
106. S. Höhna, M. J. Landis, T. A. Heath, B. Boussau, N. Lartillot, B. R. Moore, J. P. Huelsenbeck, F. Ronquist, RevBayes: Bayesian phylogenetic inference using graphical models and an interactive model-specification language. *Syst. Biol.* **65**, 726–736 (2016).
107. H. K. Voris, Maps of Pleistocene sea levels in Southeast Asia: Shorelines, river systems and time durations. *J. Biogeogr.* **27**, 1153–1167 (2000).
108. R. Hall, Southeast Asia's changing palaeogeography. *Blumea - Biodivers. Evol. Biogeogr. Plants* **54**, 148–161 (2009).
109. D. J. Lohman, M. De Bruyn, T. Page, K. Von Rintelen, R. Hall, P. K. L. Ng, H.-T. Shih, G. R. Carvalho, T. Von Rintelen, Biogeography of the Indo-Australian Archipelago. *Annu. Rev. Ecol. Evol. Syst.* **42**, 205–226 (2011).
110. D. M. Crayn, C. Costion, M. G. Harrington, The Sahul–Sunda floristic exchange: Dated molecular phylogenies document Cenozoic intercontinental dispersal dynamics. *J. Biogeogr.* **42**, 11–24 (2015).
111. A. Antonelli, W. D. Kissling, S. G. A. Flantua, M. A. Bermúdez, A. Mulch, A. N. Muellner-Riehl, H. Kreft, H. P. Linder, C. Badgley, J. Fjeldså, S. A. Fritz, C. Rahbek, F. Herman, H. Hooghiemstra, C. Hoorn, Geological and climatic influences on mountain biodiversity. *Nat. Geosci.* **11**, 718–725 (2018).
112. M. A. Iturralde-Vinent, R. D. E. MacPhee, Paleogeography of the Caribbean region: Implications for Cenozoic biogeography. *Bull. Am. Mus. Nat. Hist.* **238**, 1–95 (1999).
113. M. Storey, J. J. Mahoney, A. D. Saunders, R. A. Duncan, S. P. Kelley, M. F. Coffin, Timing of hot spot—Related volcanism and the breakup of Madagascar and India. *Science* **267**, 852–855 (1995).
114. W. L. Crepet, K. C. Nixon, M. A. Gandolfo, An extinct calycanthoid taxon, *Jerseyanthus calycanthoides*, from the Late Cretaceous of New Jersey. *Am. J. Bot.* **92**, 1475–1485 (2005).
115. J. A. Doyle, P. K. Endress, Integrating Cretaceous fossils into the phylogeny of living angiosperms: Fossil Magnoliales and their evolutionary implications. *Int. J. Plant Sci.* **185**, 42–70 (2024).
116. H. Sauquet, S. Ramírez-Barahona, S. Magallón, What is the age of flowering plants? *J. Exp. Bot.* **73**, 3840–3853 (2022).
117. S. Abadi, D. Azouri, T. Pupko, I. Mayrose, Model selection may not be a mandatory step for phylogeny reconstruction. *Nat. Commun.* **10**, 934 (2019).

Downloaded from https://www.science.org on October 08, 2026

118. C. M. Voloch, C. G. Schrago, Impact of the partitioning scheme on divergence times inferred from mammalian genomic data sets. *Evol. Bioinform.* **8**, 10.4137/EBO.S9627 (2012).
119. C. S. P. Foster, S. Y. W. Ho, Strategies for partitioning clock models in phylogenomic dating: Application to the angiosperm evolutionary timescale. *Genome Biol. Evol.* **9**, 2752–2763 (2017).
120. K. Angelis, S. Álvarez-Carretero, M. Dos Reis, Z. Yang, An evaluation of different partitioning strategies for bayesian estimation of species divergence times. *Syst. Biol.* **67**, 61–77 (2018).
121. H. Sauquet, A practical guide to molecular dating. *C. R. Palevol* **12**, 355–367 (2013).
122. D. Silvestro, N. Salamin, A. Antonelli, X. Meyer, Improved estimation of macroevolutionary rates from fossil data using a Bayesian framework. *Paleobiology* **45**, 546–570 (2019).
123. The World Flora Online Consortium, A. Elliott, R. Hyam, M. Watson, E. Wrankmore, H. Hartley, J. Krieger, K. Gandhi, R. Acuña, R. F. De Almeida, G. Amorim, G. Anderson, G. C. Andrella, M. Anguiano, H. Antonio-Domingues, W. H. Ardi, H. Atkins, J. J. Atwood, X. Aubriot, W. Baker, A. P. Balan, P. Barberá, R. Barrett, F. Bartolucci, A. M. Bedoya, W. G. Berendsohn, R. J. B. Bernal, M. Bonifacino, L. Borges, J. C. Brinda, G. Brown, A. Bruneau, P. Bunchalee, M. T. Buril, F. N. Cabral, M. Calonje, R. Camfield, F. F. M. Capelo, D. Cardoso, C. S. De Carvalho, L. Chatrou, J. Chen, F. Chiarini, L. M. Choo, J. I. M. Corro, D. S. Costa, T. L. P. Couvreur, Q. Cronk, D. Crowley, A. Culham, I. Darbyshire, M. G. Declercq, V. L. Denardi, M. Dillenberger, R. V. Docot, L. Duan, J. Dupin, J. D. T. Durán, A. N. Egan, A. Elvebakk, R. H. J. Erkens, E. V. Escallón, L. Eserman, A. Espejo-Serna, M. de la Estrella, M. Falcão, P. P. A. Ferreira, A. Franck, P. Fritsch, P. H. Gaem, E. Gagnon, G. Galasso, G. G. Del Galdo, D. German, L. Giacomin, D. Girmansyah, D. S. Gissi, H. Gladitsch, P. Gonzáles, Y. Gouvêa, R. H. A. Govaerts, B. Gregório, P. C. Guerrero, L. Haegi, T. Haevermans, M. Hanes, D. J. Harris, R. F. Hilario, H. F. Hopkins, S. Hopper, D. Hoyos, L. Hu, G. Huerta-Ramos, M. Hughes, J. Iganci, J. G. Rando, O. A. Jara-Muñoz, F. Javadi, P. R. Jennert, K.-W. Jiang, P. Jiménez-Mejías, D. Johnson, L. S. B. Jordão, H. Keller, M. Kiefer, N. Kilian, B. Klitgaard, R. R. Klopper, S. Knapp, M. Koch, N. Korotkova, K. Koutroumpa, M. Köhler, I. Larridon, N. Lavandero, M. Lavin, J. Leong-Škorničková, B. Lepschi, G. Lewis, S. Liede-Schumann, A. G. De Lima, D. F. Lima, J. C. Lopes, Y. W. Low, E. Lucas, M. Luján, M. A. Herrera-Pacheco, P. Maas, K. Mahon, L. C. Majure, M. Malekmohammadi, Y. Mambrasar, L. Marasinghe, L. C. Marinho, C. Martine, B. Maslin, O. Maurin, R. B. Melchor-Castro, S. Von Mering, D. Metzing, U. Meve, J. T. Miller, R. E. Miller, M. Moeller, A. K. Monro, T. C. E. Monteiro, P. Moonlight, I. Morais, J. F. Morales, A. L. D. C. Moreira, A. Moreira-Muñoz, A. Muellner-Riehl, D. Murphy, W. A. Mustaqim, P. Muñoz-Rodríguez, A. Müller, C. Nelson, A. Nersesyan, M. Newman, J. Nitta, M. I. U. De Oliveira, A. Orejuela, A. E. Ortiz-Rodriguez, R. Osborne, A. Pandey, M. O. O. Pellegrini, C. A. Pendry, T. Pennington, F. S. Petrongari, F. F. Pezzini, Y. Pillon, R. Pinto, M. D. Pirie, P. Poczai, A. D. Poulsen, C. Puglisi, T. L. Péchon, L. P. De Queiroz, A. Quintanar, R. K. Rabeler, H. Rainer, N. Rakotonirina, G. Ramos, D. Rankin, A. Rapini, P. Rattanakrajang, E. O. Ravomanana, L. Raz, M. Rodda, R. S. Rodrigues, B. M. Rojas-Andrés, C. Rothfels, M. M. L. Roux, V. D. S. Sampaio, L. Santilli, M. F. Santos, B. Schlumpberger, H. Schneider, J. V. Schneider, E. Schuettpelz, W. W. Seah, G. Shimizu, R. C. Silva, M. Simon, R. Simão-Bianchini, A. R. Simões, C. Skema, S. Smith, D. Sokoloff, S. Sotuyo, D. Stevenson, C. Stirton, S. Straub, J. S. Strijk, P. W. Sweeney, D. Sánchez, T. Särkinen, M. Tamayo, M. Tebbitt, E. Tepe, D. C. Thomas, A. H. Thornhill, M. Thulin, R. Trad, A. Trias-Blasi, K. S. Valdemarin, T. Vasconcelos, M. S. Vorontsova, H. F. Wang, C. Webb, L. V. V. Wedel, N. Wilding, H. Wilson, S. Winslow, P. Zamora-Tavares, C. F. Zhang, R. Zhang, G. Zizka, World Flora Online Plant List June 2025, Zenodo (2025); https://zenodo.org/records/15704590.
124. P. J. M. Maas, L. Y. T. Westra, S. A. Guerrero, A. Q. Lobão, U. Scharf, N. A. Zamora, R. H. J. Erkens, Confronting a morphological nightmare: Revision of the Neotropical genus *Guatteria* (Annonaceae). *Blumea - Biodivers. Evol. Biogeogr. Plants* **60**, 1–219 (2015).
125. P. J. M. Maas, L. Y. T. Westra, H. Rainer, U. Scharf, H. Maas-Van De Kamer, R. H. J. Erkens, T. Van Andel, S. Arias Guerrero, *Annonaceae—Flora of Guyana, Suriname and French Guiana* (Publications scientifiques du Muséum, IRD, 2023).
126. P. H. Hoekstra, J. J. Wieringa, J. M. Maas, L. W. Chatrou, Revision of the African species of *Monanthotaxis* (Annonaceae). *Blumea* **66**, 107–221 (2021).
127. T. L. P. Couvreur, L.-P. M. J. Dagallier, F. Crozier, J.-P. Ghogue, P. H. Hoekstra, N. G. Kamdem, D. M. Johnson, N. A. Murray, B. Sonké, Flora of Cameroon—Annonaceae Vol 45. *PhytoKeys* **207**, 1–532 (2022).
128. D. M. Johnson, N. A. Murray, *Flora of Thailand: Annonaceae* (Forest Herbarium, Royal Forest Department, 2022).
129. X. Li, Y. Hu, J. Guo, J. Lan, Q. Lin, X. Bao, S. Yuan, M. Wei, Z. Li, K. Man, Z. Yin, J. Han, J. Zhang, C. Zhu, Z. Zhao, Y. Liu, J. Yang, J. Nie, A high-resolution climate simulation dataset for the past 540 million years. *Sci. Data* **9**, 371 (2022).
130. K. G. Miller, M. A. Kominz, J. V. Browning, J. D. Wright, G. S. Mountain, M. E. Katz, P. J. Sugarman, B. S. Cramer, N. Christie-Blick, S. F. Pekar, The Phanerozoic record of global sea-level change. *Science* **310**, 1293–1298 (2005).
131. J. S. Antal, N. Awasthi, Fossil flora from the Himalayan foothills of Darjeeling District, West Bengal and its palaeoecological and phytogeographical significance. *J. Palaeosci.* **42**, 14–60 (1993).
132. J. S. Antal, M. Prasad, Leaf impressions of Polyalthia Bl. in the Siwalik sediments of Darjeeling District, West Bengal. *Geophytology* **26**, 125–127 (1996).
133. M. L. As-Saruri, P. J. Whybrow, M. E. Collinson, "Geology, fruits, seeds, and vertebrates (? Sirenia) from the Kaninah Formation (Middle Eocene), Republic of Yemen," in *Fossil Vertebrates of Arabia: With Emphasis on the Late Miocene Faunas, Geology, and Palaeoenvironments of the Emirate of Abu Dhabi, United Arab Emirates*, P. J. Whybrow, A. Hill, Eds. (Yale Univ. Press, 1999), pp. 443–453.
134. O. M. Ball, A contribution to the paleobotany of the Eocene of Texas. *Bull. Agric. Mech. Coll. Tex.* **2**, 1–173 (1931).
135. E. W. Berry, The fossil plants from Vero. *Florida. J. Geol.* **25**, 661–666 (1917).
136. E. W. Berry, The Lower Eocene Floras of Southeastern North America, *U.S. Geol. Surv. Prof. Pap. 91* (US Government Printing Office, Washington, DC, 1916), pp. 481.
137. E. W. Berry, Miocene fossil plants from northern Peru. *Proc. U. S. Natl. Mus.* **55**, 279–294 (1919).
138. E. W. Berry, Tertiary fossil plants from Costa Rica. *Proc. U. S. Natl. Mus.* **59**, 169–185 (1921).
139. E. W. Berry, Miocene plants from southern Mexico. *Proc. U. S. Natl. Mus.* **62**, 1–27 (1923).
140. E. W. Berry, Petrified fruits and seeds from the Oligocene of Peru. *Pan-Am. Geol.* **47**, 121–132 (1927).
141. E. W. Berry, Tertiary fossil plants from the Argentine Republic. *Proc. U. S. Natl. Mus.* **73**, 1–27 (1928).
142. E. W. Berry, Fossil fruits in the Ancon Sandstone of Ecuador. *J. Paleo.* **3**, 298–301 (1929).
143. E. W. Berry, Revision of the Lower Eocene Wilcox flora of the southeastern States, with descriptions of new species, chiefly from Tennessee and Kentucky. *U.S. Geol. Surv. Prof. Pap.* **156**, 1–196 (1930).
144. E. W. Berry, Tertiary plants from Venezuela. *Proc. U. S. Natl. Mus.* **83**, 335–360 (1936).
145. S. D. Bonde, Unonaspermum corneri gen. et sp. nov., an annonaceous seed from the Deccan Intertrappean beds of India. *J. Indian Bot. Soc.* **72**, 251–253 (1993).
146. R. W. Brown, "Paleocene flora of the Rocky Mountains and Great Plains" (U.S. Geol. Surv. Prof. Pap. 375, 1962).
147. M. E. J. Chandler, Some Upper Cretaceous and Eocene fruits from Egypt. *Bull. Br. Mus. Nat. Hist. Geol.* **2**, 149–187 (1954).
148. M. E. J. Chandler, Palaeocene Floras: London Clay Flora (Supplement), vol 1 of *The Lower Tertiary Floras of Southern England* (British Museum Natural History, 1961).
149. M. E. J. Chandler, *A Summary and Survey of Findings in the Light of Recent Botanical Observations*, vol. 4 of *The Lower Tertiary Floras of Southern England* (British Museum Natural History, 1964).
150. M. E. J. Chandler, Supplement to the Lower Tertiary Floras of Southern England, part 5. *Tert. Res. Spec. Pap.* **4**, 1–47 (1978).
151. R. W. Chaney, E. I. Sanborn, The Goshen flora of west central Oregon. *Publ. Carnegie Inst. Wash.* **439**, 1–103 (1933).
152. K. I. Chesters, The Miocene flora of Rusinga Island, Lake Victoria, Kenya. *Palaeontographica* **101**, 30–71 (1957).
153. K. Chesters, LXI.—Some plant remains from the Upper Cretaceous and tertiary of West Africa. *J. Nat. Hist.* **8**, 498–504 (1955).
154. T. D. A. Cockerell, Descriptions of tertiary plants, II. *Am. J. Sci.* **26**, 537–544 (1908).
155. M. E. Collinson, *Fossil Plants of the London Clay* (Palaeontological Association, 1983).
156. M. Crawley, *Angiosperm Woods from British Lower Cretaceous and Palaeogene Deposits* (Palaeontological Association, 2001).
157. D. L. Dilcher, T. A. Lott, A middle Eocene fossil plant assemblage (Powers Clay Pit) from western Tennessee. *Bull. Florida Mus. Nat. Hist.* **45**, 1–43 (2005).
158. H. Engelhardt, *Ueber tertiäre Pflanzen von Chile* (Frankfurt, 1891). [On Tertiary plants of Chile.]
159. F. Geissert, H. J. Gregor, D. H. Mai, W. Boenigk, T. Guenther, Die "Saugbaggerflora", eine Frucht- und Samenflora aus dem Grenzbereich Miozän–Pliozän von Sessenheim im Elsass (Frankreich). *Doc. Nat.* **57**, 1–207 (1990). [The "suction-dredge flora," a fruit and seed flora from the Miocene–Pliocene boundary of Sessenheim, Alsace, France.]
160. A. Hollick, E. W. Berry, A late Tertiary flora from Bahia, Brazil. *Johns Hopkins Univ. Stud. Geol.* **5**, 1–136 (1924).
161. R. S. Irving, T. F. Stuessy, A new paratropical angiosperm florule in the Eocene Rockdale Formation of Bastrop County, Texas. *Southwest. Nat.* **16**, 111–116 (1971).
162. B. F. Jacobs, C. H. S. Kabuye, A Middle Miocene (12.2 My old) forest in the East African Rift Valley, Kenya. *J. Hum. Evol.* **16**, 147–155 (1987).
163. M. Konomatsu, N. Awasthi, Plant fossils from Arung Khola and Binai Khola formations of Churia Group (Siwalik), west-central Nepal and their palaeoecological and phytogeographical significance. *J. Palaeosci.* **48**, 163–181 (1999).
164. R. Kowalski, Miocene carpological floras of the Konin region (Central Poland). *Acta Palaeobot.* **57**, 39–100 (2017).
165. R. N. Lakhanpal, "Fossil Fissistigma from the Lower Siwalik near Jawalamukhi, India," in *J. Sen Memorial Volume*, H. Santapau, A. K. Ghosh, S. Chanda, S. K. Roy, S. K. Chaudhuri, Eds. (Botanical Society of Bengal, 1969), pp. 311–312.

Downloaded from https://www.science.org on October 08, 2026

166. Y. S. Liu, S. X. Guo, D. K. Ferguson, Catalogue of Cenozoic megafossil plants in China. *Palaeontogr. Abt. B* **238**, 141–179 (1996).
167. D. H. Mai, R. Givulescu, Zur Kenntnis fossiler Asimina-Samen (Anonaceae) in Europa. *Rev. Roum. Géol. Géophys. Géogr., Sér. Géol.* **20**, 277–281 (1976).
168. S. R. Manchester, F. Herrera, E. Fourtanier, J. Barron, J.-N. Martinez, Oligocene age of the classic Belén fruit and seed assemblage of north coastal Peru based on diatom biostratigraphy. *J. Geol.* **120**, 467–476 (2012).
169. D. J. Peppe, J. M. Erickson, L. J. Hickey, Fossil leaf species from the Fox Hills Formation (Upper Cretaceous: North Dakota, USA) and their paleogeographic significance. *J. Paleontol.* **81**, 550–567 (2007).
170. U. Prakash, Fossil woods from the Lower Siwalik beds of Uttar Pradesh, India. *Palaeobotanist* **25**, 376–392 (1976).
171. M. Prasad, Siwalik (Middle Miocene) leaf impressions from the foothills of the Himalayas, India. *Tert. Res.* **15**, 53–90 (1994).
172. M. Prasad, Angiospermous fossil leaves from the Siwalik foreland basins and their palaeoclimatic implications. *J. Palaeosci.* **57**, 177–215 (2008).
173. M. Prasad, Alok, A. K. Kannaujia, S. Kumar, S. K. Singh, Middle Miocene flora from Siwalik foreland basin of Uttarakhand, India and its phytogeographic and palaeoclimatic implications. *Palaeobotanist* **66**, 223–312 (2017).
174. M. Prasad, J. S. Antal, V. D. Tiwari, Investigation on plant fossils from Seria Naka in the Himalayan foothills of Uttar Pradesh, India. *Palaeobotanist* **46**, 13–30 (1997).
175. M. Prasad, J. S. Antal, P. P. Tripathi, V. K. Pandey, Further contribution to the Siwalik flora from the Koilabas area, western Nepal. *Palaeobotanist* **48**, 49–95 (1999).
176. M. Prasad, N. Awasthi, Contribution to the Siwalik flora from Surai Khola sequence, western Nepal and its palaeoecological and phytogeographical implications. *Palaeobotanist* **43**, 1–42 (1994).
177. M. Prasad, R. Ghosh, P. P. Tripathi, Floristics and climate during Siwalik (Middle Miocene) near Kathgodam in the Himalayan foothills of Uttarakhand, India. *J. Palaeontol. Soc. India* **49**, 35–93 (2004).
178. M. Prasad, H. Singh, S. K. Singh, Early Eocene Annona fossils from Vastan Lignite Mine, Surat district, Gujarat, India: Age, origin and palaeogeographic significance. *Curr. Sci.* **107**, 1730–1735 (2014).
179. M. Prasad, P. P. Tripathi, Plant megafossils from the Siwalik sediments of Bhutan and their climatic significance. *Biol. Memoirs* **26**, 6–19 (2000).
180. K. Rásky, Fosszilis növénymaradványok a dunántúli alsóeocénben (Fossil plant remains from the Lower Eocene of Transdanubia, Hungary). *Bull. Hung. Geol. Soc.* **86**, 291–294 (1956).
181. E. M. Reid, M. E. J. Chandler, *The London Clay Flora* (British Museum Natural History, 1933).
182. J. L. Roth, "Epidermal studies in the Annonaceae and related families," thesis, Indiana University, Bloomington (1981).
183. M. Salard-Cheboldaeff, Sur la palynoflore maastrichtienne et tertiaire du bassin sédimentaire littoral du Cameroun. *Pollen Spores* **20**, 215–260 (1978). [On the Maastrichtian and Tertiary palynoflora of the coastal sedimentary basin of Cameroon.]
184. P. S. Shashi, P. P. Tripathi, Siwalik (Middle Miocene) leaf impressions from Tanakpur area, Uttarakhand and their bearing on climate. *Geophytology* **37**, 99–108 (2008).
185. S. M. P. Shashi, P. P. Tripathi, Fossil leaf impressions from Siwalik sediments of the Himalayan foothills of Uttarakhand, India and their significance. *J. Palaeosci.* **55**, 77–87 (2006).
186. A. Shukla, R. C. Mehrotra, Paleoequatorial rain forest of western India during the EECO: Evidence from a *Uvaria* L. fossil and its geological distribution pattern. *Hist. Biol.* **26**, 693–698 (2014).
187. H. Singh, M. Prasad, K. Kumar, S. K. Singh, Paleobotanical remains from the Paleocene–lower Eocene Vagadkhol Formation, western India and their paleoclimatic and phytogeographic implications. *Palaeoworld* **20**, 332–356 (2011).
188. E. A. A. Soares, A. C. Kloster, S. C. Gnaedinger, S. R. Riker, F. J. da Cruz Lima, M. B. Motta, First record of Annonaceae wood for the Neogene of South America, Amazon Basin, Brazil. *Braz. J. Geol.* **47**, 95–108 (2017).
189. J. R. Tao, Ed., *The Evolution of the Late Cretaceous–Cenozoic Floras in China* (Science Press, 2000).
190. B. H. Tiffney, J. G. Fleagle, T. M. Bown, Early to Middle Miocene angiosperm fruits and seeds from Fejej, Ethiopia. *Tert. Res.* **15**, 25–42 (1994).
191. B. H. Tiffney, J. U. McClammer Jr., A seed of the Anonaceae from the Palaeocene of Pakistan. *Tert. Res.* **9**, 13–20 (1988).
192. P. P. Tripathi, S. M. Pandey, M. Prasad, Angiospermous leaf impressions from the Siwalik sediments of the Himalayan foothills near Jarwa, Uttar Pradesh, and their palaeoclimatic significance. *Biol. Mem.* **28**, 79–90 (2002).
193. J. van der Burgh, Miocene floras in the Lower Rhenish Basin and their ecological interpretation. *Rev. Palaeobot. Palynol.* **52**, 299–366 (1987).
194. H. Wang, J. Blanchard, D. L. Dilcher, Fruits, seeds, and flowers from the Warman clay pit (Middle Eocene Claiborne Group), western Tennessee, USA. *Palaeontol. Electron.* **16**, 31A (2013).
195. E. A. Wheeler, S. R. Manchester, Woods of the Middle Eocene nut beds flora, Clarno Formation, Oregon, USA. *IAWA J. Suppl.* **3**, 1–188 (2002).
196. G. Srivastava, R. C. Mehrotra, First fossil record of Alphonsea Hk. f. & T. (Annonaceae) from the Late Oligocene sediments of Assam, India and comments on its phytogeography. *PLOS ONE* **8**, e53177 (2013).
197. R. N. Lakhanpal, The Rujada flora of west-central Oregon. *Univ. Calif. Publ. Geol. Sci.* **35**, 1–66 (1958).
198. S. R. Manchester, Fruits and seeds of the Middle Eocene nut beds flora, Clarno Formation. *Oregon. Palaeontogr. Am.* **58**, 1–205 (1994).
199. M. E. J. Chandler, *Flora of the Bournemouth Beds: The Boscombe and the Highcliff Sands*, vol. 3 of *The Lower Tertiary Floras of Southern England* (British Museum Natural History, 1963).
200. N. Solé de Porta, Algunos géneros nuevos de polen procedentes de la Formación Guaduas (Maastrichtiense–Paleoceno) de Colombia. *Stud. Geol. Salmant.* **2**, 133–143 (1971). [Some new pollen genera from the Guaduas Formation (Maastrichtian–Paleocene) of Colombia.]
201. J. S. Antal, M. Prasad, Morphotaxonomic study of some more fossil leaves from the Lower Siwalik sediments of West Bengal, India. *Palaeobotanist* **47**, 86–98 (1998).
202. M. Prasad, H. D. Dwivedi, Systematic study of the leaf impressions from the Churia Formation of Koilabas area, Nepal and their significance. *Palaeobotanist* **56**, 139–154 (2007).

Acknowledgments: Plant material was provided by the following herbaria: AAU, ALF, ASU, B, BKF, BM, BR, BRLU, CAL, CHOCO, CMUB, COI, COL, CUMB, CUVC, DR, EA, F, FCME, Forestry Agency St. Lucia, G, GH, GHENT, HKU, IBSC, INPA, IOU, JPB, K, L, MEXU, MO, MPU, NIT, NOU, NY, OHU, OWU, OXF, P, PSU, QCA, RB, S, SING, SP, SPF, U, UFP, US, WAG, and WU. All curators are thanked for letting us access this important material. We thank I. Quintero for advice in running INSANE, D. Silvestro for advice with PyRate parameters, N. Upham for initial feedback with the patching script, I. Turner and P. Maas for taxonomical discussions, and S. Hamdi and M. Lejbowicz for help with paperwork around the project. T. Delaigue provided technical support. We acknowledge the ISO 9001 certified IRD i-Trop HPC (South Green Platform) at IRD Montpellier for providing HPC resources that have contributed to the phylogenetic results reported within this paper. **Funding:** This project has received funding from the European Research Council (ERC) under the European Union's Horizon 2020 research and innovation program (project GLOBAL to T.L.P.C., agreement no. 865787). F.L.C. was supported by the European Research Council (ERC) under the European Union's Horizon 2020 research and innovation program (project GAIA, agreement no. 851188). **Author contributions:** F.L.C., P.S., and T.L.P.C. were involved in the conceptualization of the work. C.M., D.T., F.L.C., F.J.N., L.H., P.S., and T.L.P.C. contributed to the methodology. A.D., A.E.O.-R., S.A.G., A.T.P., J.C., C.L., C.R.-V., D.C.T., D.M.J., F.L.C., F.J.N., F.F., G.R., J.C.L., J.J.W., A.L., M.D.P., L.H., L.-P.M.J.D., L.W.C., K.M., M.L.B., N.A.M., P.B., P.H.H., R.Bo., R.Bi., R.H.J.E., T.C., T.L.P.C., and V.R.C.S. were responsible for data curation. C.M., B.S., D.C.T., D.T., F.L.C., F.J.N., J.C.L., J.J.W., J.N.Z., L.H., R.H.J.E., and T.L.P.C. carried out the investigations. C.M., D.T., F.L.C., F.J.N., G.R., L.H., and T.L.P.C. conducted formal analyses. D.T., F.J.N., L.H., S.J.R.S., and T.L.P.C. prepared the visualizations. S.A.G., C.M., C.R.-V., D.T., F.L.C., G.R., H.S., J.C.L., L.H., R.H.J.E., T.L.P.C., and V.R.C.S. provided resources. A.T.P., C.M., D.T., F.L.C., F.J.N., G.R., L.H., and T.L.P.C. developed scripts. C.M., D.T., F.L.C., F.J.N., L.H., L.W.C., and T.L.P.C. led the supervision. S.A.G., A.J.P., J.C., C.M., D.C.T., D.M.J., D.T., F.L.C., F.J.N., G.R., H.R., H.S., J.C.L., A.L., L.H., L.H.M.F., L.-P.M.J.D., M.D.P., N.A.M., P.H.H., R.H.J.E., S.J.R.S., T.C., and T.L.P.C. validated results. F.L.C. and T.L.P.C. acquired funding. T.L.P.C. administered the project. D.T., F.L.C., F.J.N., L.H., R.H.J.E., and T.L.P.C. led the writing of the original draft. All coauthors reviewed the final manuscript. **Competing interests:** The authors declare that they have no competing interests. **Data, code, and materials availability:** All data and code needed to evaluate and reproduce the results in the paper are present in the paper and/or the Supplementary Materials. In addition, additional datasets and scripts have been deposited on Dryad (DOI: 10.5061/dryad.w6m905r27). We generated a searchable online database to access voucher information for sequenced specimens (https://global.ird.fr/app/). This study did not generate new materials.

Submitted 3 December 2025
Accepted 26 August 2026
Published 30 September 2026
10.1126/sciadv.aee4197

Downloaded from https://www.science.org on October 08, 2026

ScienceAdvances

Macroevolutionary dynamics and predictors of tropical rain forest plant diversity

Laura Holzmeyer, Francis J. Nge, Susana Arias Guerrero, Kate E. Armstrong, Márcio L. Bazante, Roxali Bijmoer, Renata Borosova, David D. Bruy, Pasakorn Bunchalee, Tanawat Chaowasku, Lars W. Chatrou, Junhao Chen, Léo-Paul M. J. Dagallier, Anissara Damthongdee, Roy H. J. Erkens, Federico Fabriani, Luiz H. M. Fonseca, Myriam Gaudeul, Paul H. Hoekstra, David M. Johnson, Thea Lautenschläger, Charan Leeratiwong, Ming-Fai Liu, Adriana A. Q. Lobão, Jenifer C. Lopes, Cedric Mariac, Maria F. Martínez-Velarde, Kathryn P. Mercier, Fabian A. Michelangeli, Rommel Montúfar, Jérôme J. Munzinger, Nancy A. Murray, Andrés E. Ortiz-Rodriguez, Álvaro J. Pérez, Michael D. Pirie, Heimo Rainer, Mijoro Rakotoarinivo, Carlos Rodrigues-Vaz, Germinal Rouhan, Hervé Sauquet, Bonaventure Sonké, Vincent R. C. Soulé, Tariq Stévart, Serafin J. R. Streiff, Joeri S. Strijk, Delphine Tardif, Daniel C. Thomas, Archimède Towe Patipe, Jan J. Wieringa, J. Nicolás Zapata, Pierre Sepulchre, Fabien L. Condamine, and Thomas L. P. Couvreur

Sci. Adv. **12** (40), eaee4197. DOI: 10.1126/sciadv.aee4197

View the article online
https://www.science.org/doi/10.1126/sciadv.aee4197
Permissions
https://www.science.org/help/reprints-and-permissions

Downloaded from https://www.science.org on October 08, 2026

Use of this article is subject to the Terms of service

Science Advances (ISSN 2375-2548) is published by the American Association for the Advancement of Science. 1200 New York Avenue NW, Washington, DC 20005. The title *Science Advances* is a registered trademark of AAAS.

Copyright © 2026 The Authors, some rights reserved; exclusive licensee American Association for the Advancement of Science. No claim to original U.S. Government Works. Distributed under a Creative Commons Attribution NonCommercial License 4.0 (CC BY-NC).